T.C.
DOKUZ EYLUL UNIVERSITY
IZMIR INTERNATIONAL BIOMEDICINE AND GENOME INSTITUTE

DEVELOPMENT OF 3D MICROFLUIDIC PLATFORM FOR *in vitro* DISEASE MODELLING OF MACULAR CORNEAL DYSTROPHY

İREM DUMAN

MOLECULAR BIOLOGY AND GENETICS

MASTER OF SCIENCES THESIS

İZMİR-2022

Thesis ID: DEU.IBG.MSc.2019850030

T.C.
DOKUZ EYLUL UNIVERSITY
IZMIR INTERNATIONAL BIOMEDICINE AND GENOME INSTITUTE

DEVELOPMENT OF 3D MICROFLUIDIC PLATFORM FOR *in vitro* DISEASE MODELLING OF MACULAR CORNEAL DYSTROPHY

MOLECULAR BIOLOGY AND GENETICS

MASTER OF SCIENCES THESIS

İREM DUMAN

Supervisor: Assoc. Prof. Dr. Sinan Güven

TÜBİTAK 318S208

(This research was supported by TÜBİTAK grand number 318S208)

THESIS ID : DEU.IBG.MSc.2019850030

Dokuz Eylül Üniversitesi İzmir Uluslararası Biyotıp ve Genom Enstitüsü Genom Bilimleri ve Moleküler Biyoteknoloji Anabilim Dalı, Moleküler Biyoloji ve Genetik Yüksek Lisans programı öğrencisi İrem Duman **"DEVELOPMENT OF 3D MICROFLUIDIC PLATFORM FOR IN VITRO DISEASE MODELLING OF MACULAR CORNEAL DYSTROPHY"** konulu Yüksek Lisans tezini 25.05.2022 tarihinde başarılı olarak tamamlamıştır.

BAŞKAN
Doç. Dr. Sinan Güven
Dokuz Eylül Üniversitesi

ÜYE
Prof. Dr. Hüsnü Alper Bağrıyanık
Dokuz Eylül Üniversitesi

ÜYE
Dr. Öğr. Üyesi Burçak Alp
İzmir Ekonomi Üniversitesi

YEDEK ÜYE
Prof. Dr. Gülgün Oktay
Dokuz Eylül Üniversitesi

YEDEK ÜYE
Doç. Dr. Cumhur Tekin
İzmir Yüksek Teknoloji Ensititüsü

Dokuz Eylul University Izmir International Biomedicine and Genome Institute Department of Genomics and Molecular Biotechnology, Molecular Biology and Genetics graduate program Master of Science student İrem Duman has successfully completed her Master of Science thesis titled **"DEVELOPMENT OF 3D MICROFLUIDIC FOR PLATFORM IN VITRO DISEASE MODELLING OF MACULAR CORNEAL DYSTROPHY"** on the date of 25.05.2022.

CHAIR

Assoc. Prof. Dr. Sinan Güven

Dokuz Eylul University

MEMBER

Prof. Dr. Hüsnü Alper Bağrıyanık

Dokuz Eylul University

MEMBER

Asst. Prof. Burçak Alp

Izmir University of Economics

SUBSTITUTE MEMBER

Prof. Dr. Gülgün Oktay

Dokuz Eylul University

SUBSTITUTE MEMBER

Assoc. Prof. Dr. Cumhur Tekin

Izmir Institute of Technology

Table of Contents

Index of Tables

Index of Figures

List of Abbreviations

2D	2-Dimensional
3D	3-Dimensional
ALDH1A1	Aldehyde Dehydrogenase 1 Family Member A1
ALDH3A1	Aldehyde Dehydrogenase 3 Family Member A1
APS	Ammonium Persulfate
BSA	Bovine Serum Albumin
CHST6	Carbohydrate Sulfotransferase 6
DALK	Deep Anterior Lamellar Keratoplasty
DEC	Decorin
DKSFM	Defined Keratinocyte Serum Free Medium
DMEM	Dulbecco's Modified Eagle Medium
DMSO	Dimethyl Sulfoxide
ECM	Extracellular Matrix
EDC	N′-ethylcarbodiimide hydrochloride
FBS	Fetal Bovine Serum
GAG	Glycosaminoglycan
HCl	Hydrochloric Acid
HMDS	Hexamethyldisilazane
IC3D	The International Committee for Classification of Corneal Dystrophies
ICC	Immunocytochemistry
IHC	Immunohistochemistry

KSPGs	Keratan Sulfate Proteoglycans
LUM	Lumican
MCD	Macular Corneal Dystrophy
MES	2-(N-Morpholino)ethanesulfonic acid
MIM	Mimecan
MMP-1	Matrix Metalloproteinase-1
MMP-13	Matrix Metalloproteinase-13
MPC	2-methacryloxy-ethyl phosphorylcholine
$NaClO_3$	Sodium Chlorate
NHS	N-Hydroxysuccinimide
PAPs	3′-phosphoadenosine-5′-phosphosulfate
PBS	Phospate Buffered Saline
PDMS	Polydimethylsiloxane
PEG	Poly(ethylene Glycol)
PEGDA	Poly(ethylene Glycol Diacrylate)
PFA	Paraformaldehyde
PGs	Proteoglycans
PI	Propidium Iodide
PMMA	Poly(methyl methacrylate)
PS	Pen Strep
PVA	Poly Vinyl Alcohol
SEM	Scanning Electron Microscopy
TEMED	N,N,N,Ntetramethylethylenediamine

TIMP1	Tissue inhibitor of metalloproteinases 1
TIMP2	Tissue inhibitor of metalloproteinases 2

ACKNOWLEDGEMENTS

First and foremost, I want to express my gratitude to Assoc. Prof. Sinan Güven, my thesis advisor, for his unwavering support, advice, and patience. He is always there for me whenever I need him, and he has taught me how to think scientifically and how to express myself professionally.

Apart from my advisor, I'd like to express my gratitude to Dr. Canan Aslı Yıldırım for her insightful suggestions. I'd want to express my appreciation to Nevin Ersoy, Defne Öztürk, Ece Uzun, and all IBG core facilities members for their support and friendship. I'd like to thank Abdullah Eyidoğan for his help, as well as TUBITAK for supporting this study.

I thank all of my lab members in the Therapeutic Bioengineering Group and my friends, especially Sude Uyulgan, who was always there for me with her unwavering patience and endless song performances, Tugba Topbaş, who was always there for me and helped me in any situation without hesitation, Nevin Ersoy has always been willing to answer my questions and share her experiences with me, and she has always been supportive of me, Vedat Sarı and his amazing coffee during experiment breaks, Elifsu Polatlı, and Alican Koç for their unending support and friendship. I also would like to thank Cansu Bayram for her unconditional love, patience, making me confidentand motivated again after long working days.

Last but not least, I'd want to dedicate this thesis to my parents and my brother, Emre Taylan Duman, who has been my biggest supporter and hero throughout this process. Without him, I would not have been able to complete this thesis or get through difficult circumstances in my life.

DEVELOPMENT OF 3D MICROFLUIDIC PLATFORM *in vitro* DISEASE MODELLING OF MACULAR CORNEAL DYSTROPHY

İrem Duman, Izmir International Biomedicine and Genome Institute, Dokuz Eylul University 15 Temmuz Health and Art Campus, Balcova, 35340, Izmir/Turkey

ABSTRACT

Cornea is an avascular structure that provides refraction, transparency, and protects the eye's anterior part. Collagen generates a unique tissue structure that promotes physical qualities and strengthens the rigidity of the outer eye. Corneal dystrophies are rare hereditary diseases that produce corneal defects. Macular corneal dystrophy (MCD) is an autosomal recessively inherited condition in which mutations in the CHST6 gene, which codes for the enzyme N-acetylglucosamine-6-sulfotransferase, induce aberrant proteoglycan production. Corneal opacity is caused by the accumulation of glycosaminoglycans among stroma keratocytes, resulting in visual impairment. MMP1 and MMP13 from the matrix metalloproteinase (MMP) family, which are involved in corneal remodeling, have been found to be reduced in the extracellular matrix in MCD disease. Current clinical methods are mostly focused on corneal transplants, which do not eliminate the risk of recurrence.

Here, we create a dynamic microfluidic platform to test an alternate treatment technique that includes MMP enzyme therapy in an *in vitro* model of MCD. Primary human corneal cells were extracted and planted on a hydrogel made up of mainly collagen which mimicked the biochemical and mechanical properties of the cornea. The cells were cultivated in a microfluidic platform in continuous laminar flow under dynamic conditions. We demonstrate that imitating sulfation inhibition using sodium chlorate, a pharmacological inhibitor of 3′-phosphoadenosine-5′-phosphosulfate (PAPs), results in long-term cell survival and MCD (-) related molecular responses at the gene level. The bioengineered example disease model will be a good platform for learning more about MCD and creating new treatments in clinics.

Key Words: Microfluidics, Disease Modelling, Rare Disease, Macular Corneal Dystrophy

MAKÜLER KORNEA DİSTROFİSİNİN MİKROAKIŞKAN PLATFORM İÇERİSİNDE *in vitro* HASTALIK MODELLENMESİ

İrem Duman, İzmir Uluslararası Biyotıp ve Genom Enstitüsü, Dokuz Eylül Üniversitesi 15 Temmuz Sağlık ve Sanat Kampusü, Balçova, 35340, Izmir/Turkey

ÖZET

Kornea avasküler yapısıyla gözün dış kısmını korurken kırınım ve şeffaflık sağlayarak da görmeye yardımcı olur. Bu benzersiz doku yapısı glikozaminoglikan (GAG) ve kolajenden oluşan birliktelikle gözün dış kısmının sertliğini arttırmaktadır. Kornea distrofileri korneada bazı anomalilere sebep olan çoğunlukla nadir kalıtsal hastalıklardır. Maküler kornea distrofisi (MKD), N-asetilglukosamin-6-sülfotransferaz enzimini kodlayan CHST6 genindeki mutasyonlar nedeniyle oluşan anormal proteoglikan sentezinin görüldüğü otozomal resesif kalıtılan bir hastalıktır. Stroma keratositlerinde glikozaminoglikanların birikmesi korneada opaklaşmaya ve bu da görme bozukluğuna yol açar. MKD hastalığında korneanın yeniden şekillenmesinde görevli matriks metalloproteinaz (MMP) ailesinden ekstraselüler matrikte bulunan MMP1 ve MMP13 ün azaldığı gözlemlenmiştir. Güncel klinik yaklaşımlar daha çok nüks risklerinin elimine edilemediği kornea transplantasyonları üzerinedir.

Bu çalışmada MKD'yi *in vitro* bir platformda oluşturarak mikroakışkan tekniklere hastalık modellemesi ve alternatif tedavi yaklaşımı olarak MMP enzimlerinin denenmesinin gerçekleştirilmesi amaçlanmıştır. Primer insan kornea hücreleri izole edilerek, korneanın biyokimyasal ve mekanik özelliklerini taklit eden kolajen, polietilen glikol ve 2-metakriloiloksietil fosforil kolinden oluşan biyomühendislik ürünü bir hidrojel üzerine ekilmiştir. Hücre ekili hidrojeller, göz içi basıncına benzer dinamik koşullar sağlayan polimetil metakrilat (PMMA) ve polidimetilsiloksandan (PDMS) oluşan mikroakışkan çip yapısında sürekli laminer akış altında kültür edilmiştir. Uzun süreli kültür süresiyle 3′-fosfoadenosin-5′-fosfosülfatın (PAP'lar) kimyasal bir inhibitörü olan sodyum klorat kullanılmış ve sülfatlaşma inhibisyonunu sağlanmıştır. MKD ile ilişkili moleküler yanıtlar gen seviyesinde değerlendirilmiştir. Biyomühendislik teknikleri kullanılarak oluşturulan bu örnek hastalık modeli, MKD'nin daha iyi anlaşılması ve

klinikte de kullanılabilecek alternatif yaklaşımların geliştirilmesi için uygun bir platform olacaktır.

Anahtar Kelimeler: Mikroakışkan, Hastalık Modeli, Nadir Hastalık, Maküler Korneal Distrofi

1. INTRODUCTION AND GOALS

1.1. Statement and Importance of the Problem

Cornea is a clear tissue that protects the iris, pupil, and anterior chamber of the eye. It consists of multiple layers, where each layer has its own structure, with different types and densities of collagens, elastins, fibronectins, laminins, and proteoglycans. The mechanical properties of these multiple organizational and constitutive motifs are vastly diverse. Most importantly the cornea's transparency, which allows light to flow through, is maintained by dense, regular protein packing inside a proteoglycan-rich matrix. (Blackburn et al., 2019).

Corneal dystrophies are rare hereditary diseases that cause progressive alterations in the cornea's structure (Aggarwal et al., 2018). Macular corneal dystrophy (MCD) is a visual impairment occurs due to mutations in carbohydrate sulfotransferase 6 (CHST6). The creation of several gray spots in the corneal stroma region is caused by the accumulation of abnormally sulfated keratan sulfates as a result of these alterations (Abbruzzese et al., 2004). Corneal transplantation is currently the only definitive treatment option for these patients (Di Iorio et al., 2010).

Murab et al. tried to create an *in vitro* model of MCD by imitating sulfation inhibition with sodium chlorate ($NaClO_3$), a chemical inhibitor of 3′-phosphoadenosine- 5′-phosphosulfate (PAPs) (Murab et al., 2016). As technology advances *in vitro* modelsare becoming more popular in medicine and biology, particularly because of their capacity to mimic intracellular function. Organ-on-chip models aim to produce a form of artificial tissue/organ by mimicking cell environment and cell-cell interactions. They were developed to better imitate cells' native habitats (Nikolic et al., 2018). In light of this knowledge, the goal of this research is to generate a cellular macular cornea dystrophy model within an on-chip platform utilizing 3D collagen based hydrogel carrier.

1.2. Purpose of the Research

The goal of this thesis is to mimic MCD disease inside a microfluidic platform by modeling the microenvironment with human primary cells and combining them with bioengineering techniques. Through this, we aim to observe the reaction of human primary cells to MMP1 and MMP13 enzymes within the generated disease-like microenvironment.

1.3. Hypothesis of the Research

In this study, we hypothesize that physiology of cornea stromal cells of MCD diagnosed patient could be recapitulated within the microfluidic platform by sulfation inhibition with sodium chlorate with isolated primary cell seeded collagen hydrogel.

Matrix metalloproteinase plays a function in corneal remodeling and migration of corneal stromal cells in the tissue, the expression levels of matrix metalloproteinase-1 (MMP1) and matrix metalloproteinase-13 (MMP13) enzymes have been reported to decrease in macular degenerations (Daniels et al., 2003) (Ye et al., 2000). In this study the effect of MMP1 and MMP13 stimulation on accumulation levels of proteoglycans will be tested in an *in vitro* disease model within the developed microfluidic platform. We hypothesize that MMP1 and MMP13 stimulation will facilitate the decrease in proteoglycan accumulation on generated disease model.

2. GENERAL INFORMATION

2.1. Cornea

Human eye is one of the most complicated organ in the body. It is into three sections: outer, middle, and inner. The cornea, which is located on the outside of the eye, protects it from the external threats and is responsible for refracting light and passing it to the inner section of the eye (Willoughby et al., 2010). Cornea is an avascular tissue and has 5 distinct layers; corneal epithelium, Bowman's membrane, stroma, Descemet's membrane and corneal endothelium (Figure 1) (Willoughby et al., 2010). Corneal epithelium is a transparent tissue that covers the anterior of the cornea and has a strong capacity to regenerate. Together with tears corneal epithelium serves as the first defense line for the eye (Nosrati et al., 2021) (Masterton & Ahearne, 2018). Bowman's layer is an acellular layer mainly made of collagen I and separates the

epithelium from the stroma. The corneal stroma is a transparent and thick layer made up of collagen type I, with the transparency provided by the fibrils' regular arrangement which is one of the layer's unique features. (Wilson, 2020) (Sridhar, 2018). Descemet's membrane is an acellular layer composed mainly of collagen type 4, but also fibronectin, laminin, and other proteins (Singhal et al., 2020). Corneal endothelial cells are crucial in the fluid transfer between the anterior chamber and the stroma (Tuft, S. J., and D. J. Coster, 1990).

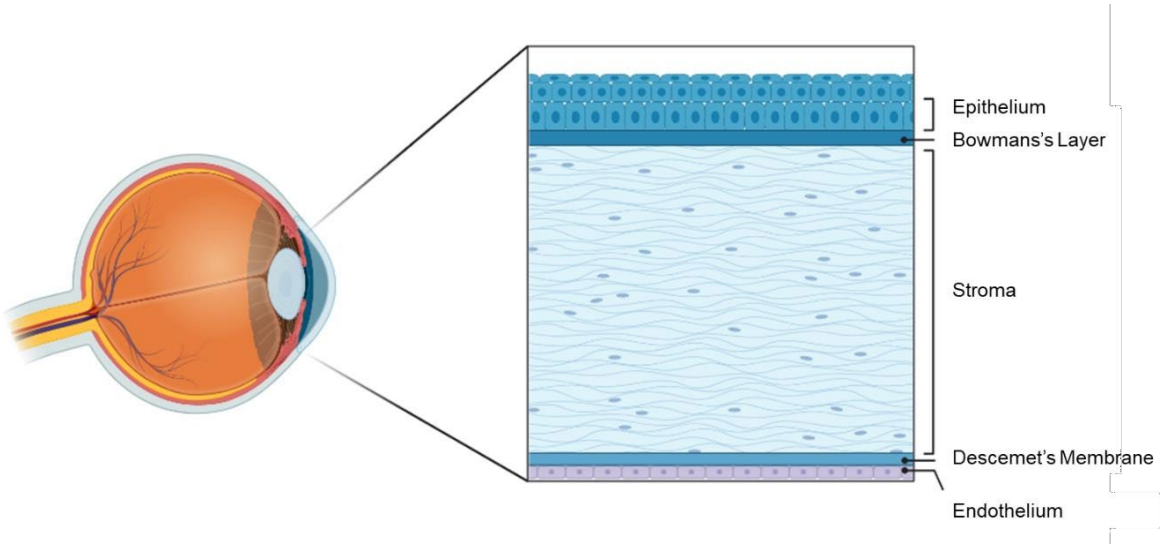

Figure 1 Layers of the cornea.

2.1.1. Corneal Stroma

The cornea stromal layer is one of the most important participants in visual function. It is located between the epithelium and the endothelial layer. The collagen fibrils, which build up the core structure are arranged in a regular pattern. This arrangement in the structure allows light to pass through the eye from cornea to retina. The cornea specific distinguished fibril architecture provides both strength and transparency (Meek & Boote, 2004).

Collagens composed 70% of the fibrous structure in the cornea. It is made up mainly by collagen I, along with other collagen types –such as II, III, V and XI- helps to create the structure (Espana & Birk, 2020). Apart from collagen, proteoglycans are another important protein that contributes to the stroma's ECM structure. Proteoglycans can be defined as structures that have several glycosaminoglycan

(GAG) chains connected to them. GAGs are polysaccharides with disaccharide groups that repeat. Decorin, lumican, keratocan, and mimecan are the proteoglycans responsible for preserving the structure and position of the fibrils in the cornea (Espana & Birk, 2020) (Baratta et al., 2022) (Michelacci, 2003). Lumican protects the ECM structure and contributes to the provision of corneal transparency by regulating the synthesis of collagen fibrils and contributing to the healing of the wound which occur in the corneal epithelial region (Zhang et al., 2017).

Normally in cornea the average size of the collagen fibrils are about the 23- 35 nm, and the triple collagen fibrils they create are around 300 nm. The arrangementand structure of the fibrils are crucial to preserving the cornea's transparency. Keratocan is another important proteoglycan that helps to keep everything in order in the cornea. In a study on mice conducted by Liu et al. it was discovered that corneal fibrils in keratocan-null animals increased in diameter and disordered (C. Y. Liu et al., 2003). Although the shape of the cornea changes depending on the situation, its transparency is also compromised (Zhang et al., 2017). Decorin and mimecan are theother two key proteoglycan that help to preserve the structure of the cornea stroma. Decorin functions in the control of interfibrillar spacing as a dermatan sulfate proteoglycan. Mimecan is a keretan sulfate proteoglycan that has a role in collagen fibril diameter regulation (Michelacci, 2003).

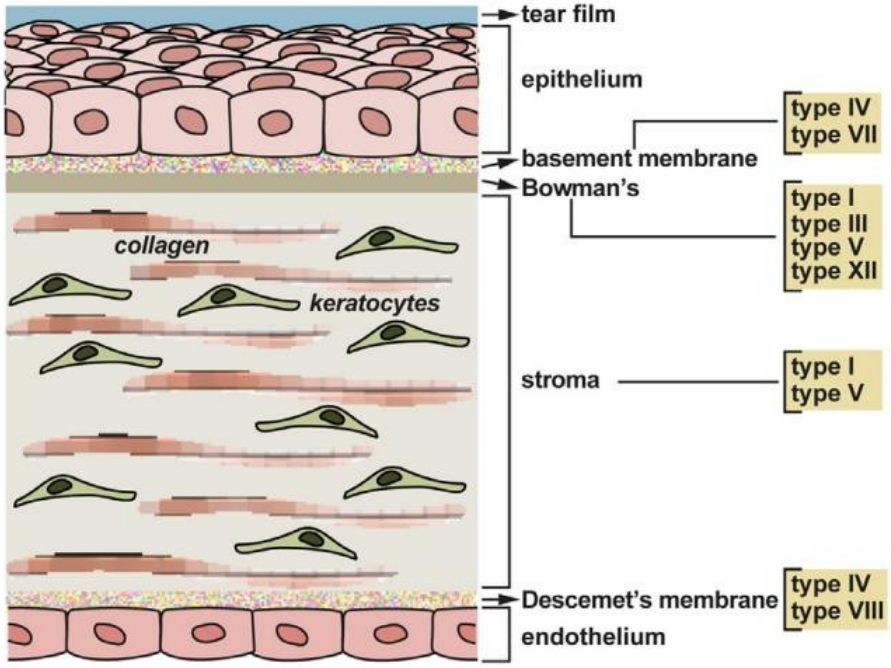

Figure 2 Cell components and collagen distribution in the cornea (Baratta et al., 2022).

Stroma layers cell component is keratocytes and these are little cells that are scattered throughout the collagen layer and play role in reducing light scattering (Figure 2). In keratinocytes, crystallins Aldehyde Dehydrogenase 3 Family Member A1 and Aldehyde Dehydrogenase 1 Family Member A1 (ALDH3A1 and ALDH1A1) are responsible for decreasing light emission and absorbing UV radiation. Keratocytes produce proteoglycans, which assist corneal transparency at the structural level, while crystallins aid this role at the intercellular level. These specific proteins, in combination with the cell surface markers CD34 and CD133, can be utilized to identify keratocytes.

2.2. Corneal Dystrophies and Macular Corneal Dystrophy (MCD)

The degeneration of the cornea's distinctive structure leads to a variety of vision-related abnormalities. Allergies, dry eye syndrome, traumas, and corneal dystrophies are just a few of the factors that can cause corneal degeneration. In medical terms, dystrophy refers to muscle diseases, and corneal dystrophy is a hereditary disorder that affects cells, tissues, or organs by acting alone or in combination with other abnormalities (Weiss et al., 2015). Corneal dystrophy is a progressive accumulation of aberrant insoluble materials in distinct layers of the cornea that can cause significant

visual impairment and vision loss up to blindness. The International Committee for Classification of Corneal Dystrophies (IC3D) standards are used to classify corneal dystrophies. This classification is based on the anatomy of the dystrophy and the amount of genetic information that has been published about it (Table 1) (Weiss et al., 2015).

Table 1 The International Committee for Classification of Corneal Dystrophies (IC3D) Categories and definitions

Category	Definition
C1	Detected the mutation and located the associated gene
C2	Mapped on one or more chromosomal loci but unidentified genes
C3	Despite the fact that it has been properly characterized, no genetic mapping has been done.
C4	Dystrophies that are suspected but not fully described

More information released about the diseases, they shift from category C4 to category C1. For the moment, it is more likely that medical treatment will be developed for diseases in category C1.

Mutations in carbohydrate sulfotransferase 6 (CHST6) induce Macular Corneal Dystrophy, which results in gray patches on the cornea (Figure 3). It causes vision impairment in its later phases. MCD is a rare autosomal recessive disease characterized by the formation of aberrant residues from unsulfated keratan sulfate proteoglycans (KSPGs). According to this information, MCD is in the C1 classification and is an autosomal recessive disease. MCD is a rare disease with an estimated prevalence of 9.7 per million people, most frequent in India, Saudi Arabia, Iceland (approximately 19 per million), and some areas of the United States (1.2 per million) (Di Iorio et al., 2010) (Klintworth, 2009).

Different surgical procedures are used to treat various corneal disorders. Some of them include penetrating keratoplasty and deep anterior lamellar keratoplasty (DALK). Although the DALK approach involves removing the corneal stroma up to the Descemet's membrane, penetrating keratoplasty refers to the replacement of a full-thickness portion of the cornea. MCD is one of the most frequent eye disease that causes corneal blindness, yet there is no solution (Keane et al., 2014) (Murab et al., 2016). DALK and penetrating keratoplasty are used to treat the condition, however there is always the potential of seeing the inherent risks of corneal transplantation and a high risk of recurrence.

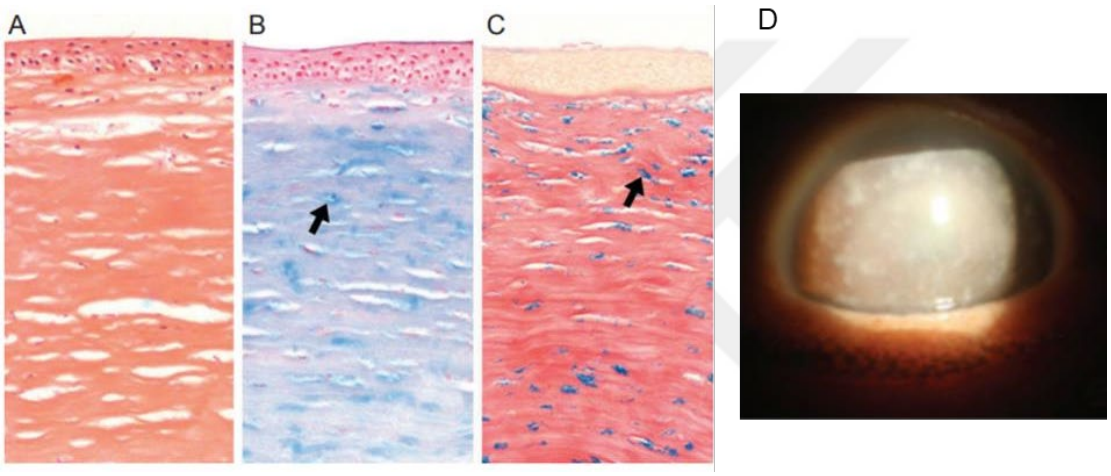

Figure 3 Histopathological staining for Macular Corneal Dystrophy A) Hematoxylin and eosin B) Alcian Blue C) Colloidal iron staining for glycosaminoglycan deposition and D) Hazy cornea (Lee et al., 2013).

Macular corneal dystrophy is divided into two main groups. MCD Type I is more common and is characterized by mutations in the CHST6 gene's coding region (Weiss et al., 2015). MCD Type II reveals deletions and rearrangements. Keratan sulfate is the most abundant glycosaminoglycan (GAG) in the cornea, and it is responsible for maintaining the cornea's hemostasis. This approach is supported by opacification of the cornea, which can occur as a result of damage or disease. In the cornea, these KS-GAG groups create proteoglycans (PGs). In MCD disease, keratan sulfate proteoglycans have no sulfate residues in their carbohydrate side chains, and second, oligosaccharide side chains in MCD (-) affected corneas are much smaller than keratan sulfate side chains found in normal corneas. Due to mutation on CHST6 gene and

these mutations negatively affect the CHST6 enzyme function this cause the impair sulfation of keratan molecules. This causes disorganization of collagen fibrils and proteoglycan accumulations, loss of transparency in the end blindness (Weiss et al., 2015) (Quantock et al., 2010) (Singh et al., 2021).

Matrix metalloproteinases (MMPs) are the major enzymes responsible for the degradation of collagen and other proteins in the extracellular matrix (Jabłońska-Trypuć et al., 2016).An increase in the levels of matrix metalloproteinase (MMPs), one of the collagen enzymes, was detected in Lumican-null mice in the study. MMP1 and MMP13 were discovered to be the enzymes that help the cornea self-stabilize (Chakravarti et al., 2000). Due to the inability of keratan sulfates to be sulfated, the downregulation of MMP1 and MMP13 in the cornea with MCD makes clearance of aberrant collagen accumulations in the stroma insufficient. Given this knowledge, it's possible that MMP1 and MMP13 enzymes, which are deficient in MCD, could be used in the treatment (Murab et al., 2016).

2.3. Biomaterials for Corneal Bioengineering

Tissue engineering is a field that combines bioengineering, biomedical engineering, and materials science, as well as the use of cell-specific components for tissue healing, treatment, and regeneration. Tissue engineering encompasses a wide range of applications and procedures for various purposes. Repairing or replacing body parts, developing a tissue scaffold for cells and using it for medicinal purposes, using hydrogels, and applying drug active compounds to tissue are just a few examples.

Currently in clinics corneal transplantation is the gold standard to approach many corneal disorders. However, post-transplantation challenges and donor shortages promote the development of bioengineering approaches in ophthalmology. Biomaterials utilized in tissue engineering and regenerative medicine should meet several features such as biocompatibility, transparency, robustness, and clinically applicable for use in the eye (Chen et al., 2018). The candidate biomaterial should not stimulate any host reaction in the patient and potentially assist regeneration and healing process. Natural and synthetic materials are both frequently used in corneal

bioengineering (Table 2). Due to the complex structure of the cornea, it is challenging to recapitulate its architecture by utilizing single type of natural or synthetic biomaterials (Palchesko et al., 2018) (Chen et al., 2018). Corneal tissue engineering strategies has been reported mostly based on natural materials such collagen, gelatin, chitosan, amniotic membrane, and silk, as well as synthetic materials like poly vinyl alcohol (PVA) and Poly(ethylene Glycol (PEG) derivatives (Table 3).

Table 2 Biomaterials for corneal bioengineering

Biomaterial	Advantages	Disadvantages
Collagen	High biocompobality	Mechanical qualities that aren't up to standard
Gelatin	Natural, cheap	Mechanical qualities that aren't up to standard
Decellularized Cornea (DC)	Similar properties to native cornea	Low bioactivity
Chitosan	Biofunctionalization is simple; biocompatibility is good; and biodegradability is manageable.	Needs to crosslink with other materials
PVA	Good mechanical properties	Other components are require to make suitable for cornea
PEGDA	Mechanical properties can be controlled	Other components are require to make suitable for cornea

Table 3 Various combination of biomaterials (Mahdavi & Abdekhodaie, 2020)

Biometarial	Advantages	Disadvantages	Clinical Status	References
Collagen + PVA	Biocompatible	Inducing inflammatory responses, lack of the expression of basement membrane components	Preclinical	Miyashita, Hideyuki, et al.
Collagen + PEGDA	Biocompatible	Inducing inflammatory responses	Preclinical	Kadakia, Arpita, et al.
Amniotic Membrane + PVA	Biocompatible, biodegradable	Inducing inflammatory responses	Preclinical	Uchino, Yuichi, et al.
Chitosan + PVA	Proper mechanical properties	Low degradation rate, Do not mimic the 3D structure of the native tissue	Basic	Seyed, Mohamed Ali; Vijayaraghavan, Kavitha.
Chitosan + PEG	Proper mechanical properties	Low degradation rate, Do not mimic the 3D structure of the native tissue	Basic	Ozcelik, Berkay, et al.

2.3.1. Collagen

Collagen is one of the most abundant elements in the body, forming bones, cartilage, fibers, and joints. It is made up of three alpha chains wrapped around each other and it has a significant role of cell adhesion, migration, and proliferation (Figure 4). It is quite popular in tissue engineering as a result of these qualities; however, it has a significant drawback in terms of mechanical durability. To overcome this drawback, it is frequently combined with cross-linkers. Type I collagen, which has the advantage of being less expensive to produce than other types, outperforms the othersin terms of strength, while type III collagen excels in terms of technical and optical characteristics (Chen et al., 2018).

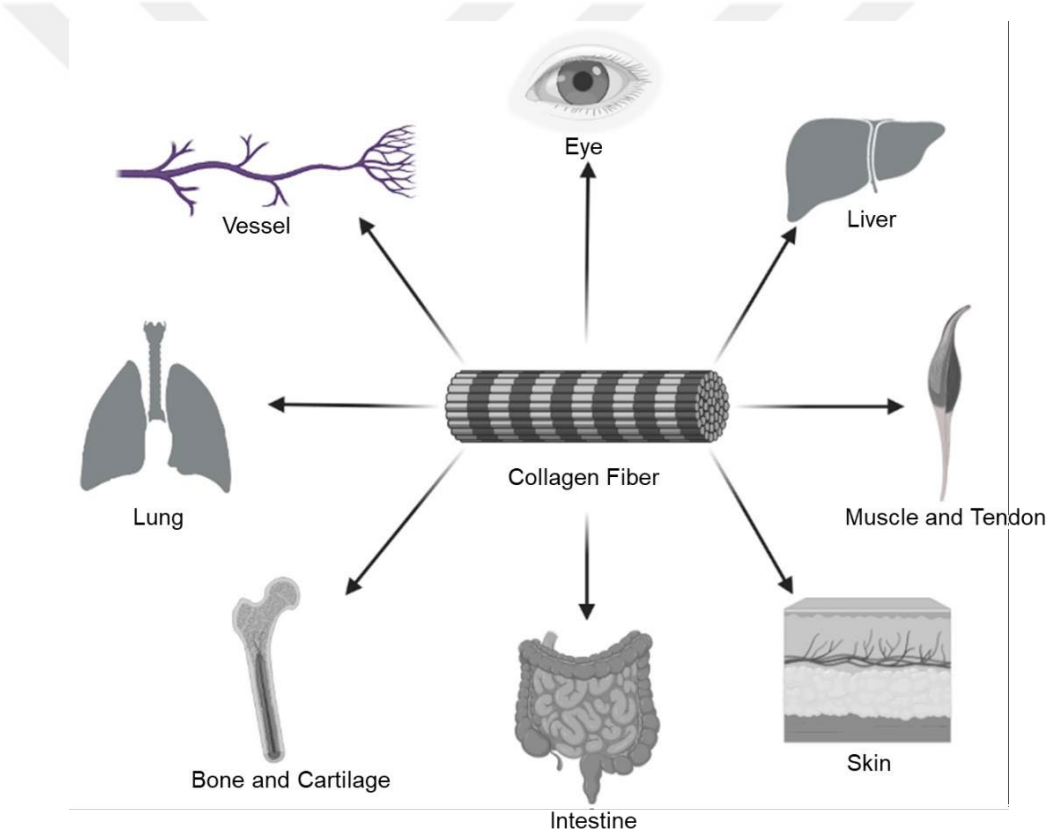

Figure 4 Collagen is found in a variety of tissues and organs throughout the body.

May Griffith and her team combined collagen I and collagen III with various cross-linkers to create an optically clear hydrogel (Islam et al., 2015). Their research focuses on collagen and its cross-linking strategies. *In vivo* investigations showed positive results for the researchers, who used collagen type I and N′-ethylcarbodiimide

hydrochloride (EDC) / N-Hydroxysuccinimide (NHS) as a crosslinker for the first time. Despite the fact that type I collagen is more common in native human corneas, they conducted the same study with collagen III, and the results were compared. They discovered that the collagen type III hydrogel had higher light transmittance than the other even though both had the same refractive index. They added (2-methacryloxy-ethyl phosphorylcholine) (MPC) chemical to increase the characteristics of the hydrogel in their subsequent investigations. With the MPC addition the hydrogel's light transmittance very near to the native cornea. In recent years, Griffith's team has completed phase I trials on these hydrogels and their research has a great potential for corneal blindness (W. Liu et al., 2008) (Y. Liu et al., 2006) (Ahn et al., 2013) (Merrett, Kimberley, et al., 2008).

2.4. Microfluidic Systems and 3D Disease Modelling

Microfluidic technology has increased in popularity in recent years, and it is providing to an analysis system that is simple to control, low cost, fast, and high sensitivity. These properties make it possible to easily control the liquids and particles inside microfluidic devices. The capacity to control the microenvironment in this way led to development of point-of-care devices, organ-on-chips, and disease models.

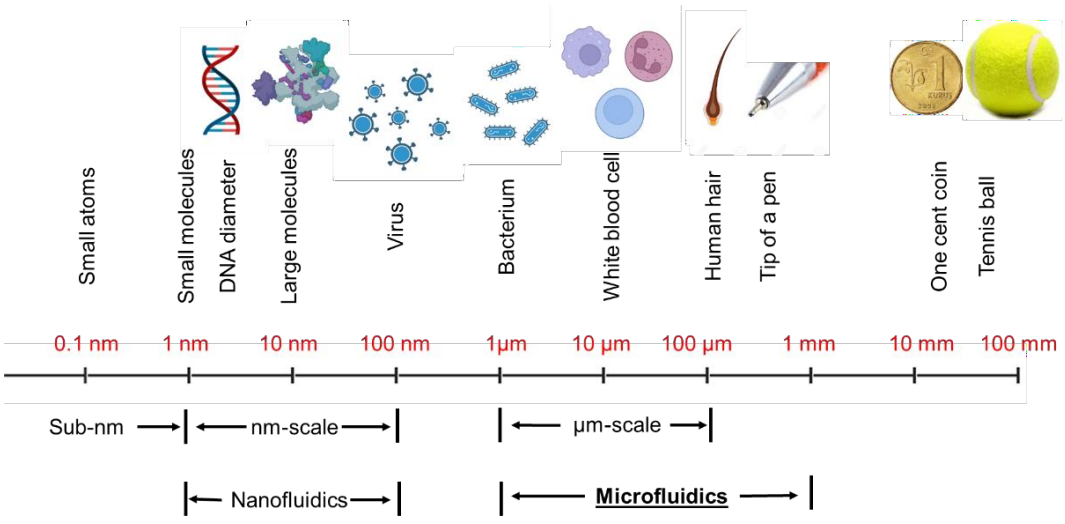

Figure 5 Scale for the microfluidic chips.

The manufacturing of microfluidic platforms involves a wide range of materials. Materials such as elastomer (Polydimethylsiloxane (PDMS)), plastic, glass, paper, and others vary depending on the necessities of the platform to be constructed (Ren et al., 2012).

Microfluidic chip systems have a wide range of applications, but when combined with bioengineering and tissue engineering disciplines, they are very beneficial for healthcare. Animals are commonly utilized, despite the fact that they are not a great model for human disease or drug toxicity tests. In vitro models, on the other hand, are not quite beneficial for representing the human body's complex structure. Organ-on-a-chip technology, which have been developed in parallel with these advancements, are an excellent platform for summarizing the complicated functionality of numerousorgans at once and building a comprehensive model of any condition. Disease modeling, therapeutic drug discovery, and personalized medicine technologies are all being developed using organ-on-a-chip technology (Jalili-firoozinezhad et al., 2021.).

In 2012, Dan Dongeun Huh and his colleagues created a lung-on-chip model, which had a huge impact in this field. On the platform, they also used the co-culture technique, which is a model for several lung disorders, particularly cystic fibrosis, with their experiments simulating the airways and breathing. In this way they've created a wonderful platform for drug studies (Figure 6) (Huh, Dongeun, et al 2012).

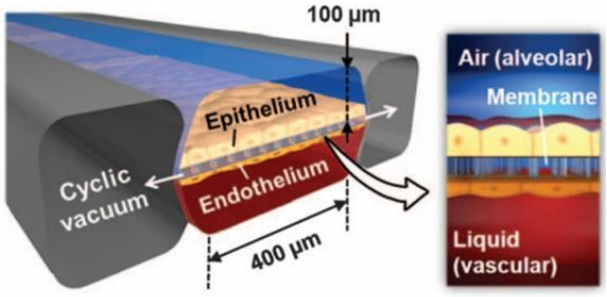

Figure 6 Representative work of lung on a chip (Huh, Dongeun, et al 2012)

In 2019, Seo and colleagues employed reverse engineering to create an eye-on-a-chip that can blink and represent the complexity of the ocular system's connection with the external environment. The major purpose in developing this system was to

replicate the most fundamental characteristics to the greatest extent possible. Cell culture is carried out in this system on a dome-shaped scaffold with three dimensions, which is one of the system's key features. At the same time, they added a tear flow and an eyelid to bring the system closer to native eye environment. Using co-culture and 3D cell patterning techniques, both sub epithelial stroma and conjunctival epithelial models created inside this system (Figure 7) (Seo et al., 2019).

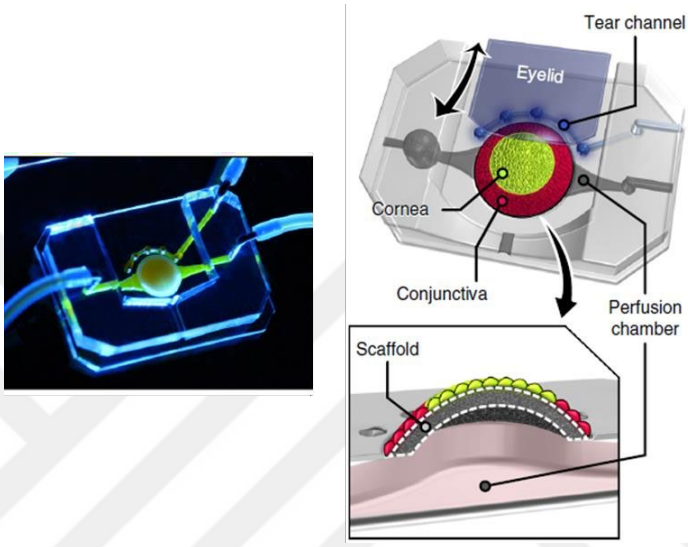

Figure 7 Representative work of bioengineered eye-on-a-chip as an *in vitro* platform for drug screening (Seo et.al., 2019).

3. MATERIALS & METHODS

3.1. Type of Research

This study encompasses *in vitro* experiments and based on cell culture techniques.

3.2. Time and Location of Research

All research was conducted between February 2020 - May 2022 at Izmir Biomedicine and Genome Center.

3.3. The Universe and Sample of Research

In this thesis human cornea samples discarded after keratinoplasty were used.

3.4. Materials of Research

In this thesis, 3T3 mouse fibroblast cells were provided by Assoc. Prof. M. Kasım Diril. Transfected GFP (+) 3T3 cells.

3.5. Variables of the Research

Independent Variables: DMEM high glucose medium, FBS and Pen-strep concentration, duration of cell culture.

Dependent Variables: structural properties of collagen based hydrogels, flow rate of microfluidic system, gene expression in protein and RNA level.

3.6. Data Collection Methods

3.6.1. 3T3 Cell Culture

3T3 cells were cultured in Dulbecco's Modified Eagle Medium (DMEM) high glucose and pyruvate (Gibco, 41966029) supplemented with high glucose medium containing 10% Fetal Bovine Serum (v/v) (FBS, Gibco, 10500064) and 1% Penicillin Streptomycin (PS).

Frozen cells were thawed in 37 °C water bath quickly to avoid damaging the cell membrane with presence of dimethyl sulfoxide (DMSO) (Sigma – Aldrich, D2650). Once cells inside the cryotube were thawed, transferred into 15 ml falcon tube which contained 3 ml of pre-warmed complete DMEM (added 10% FBS) high glucose medium. Later, cells were centrifuged at 1600 rpm for 5 min. The DMSO containing supernatant was removed. Fresh complete medium was added into the falcon tube for resuspension of the cells. 3T3 cells were seeded on 100 mm cell culture plates in complete DMEM high glucose and incubated at 37 °C incubator with 5% CO_2. Medium was refreshed within 2 or 3 days. When confluency was around 80-90%, cells were ready to be passaged.

For sub-culturing, medium was removed from 100 mm cell culture plate and cells were gently washed with 1X PBS. Then, appropriate volume of trypsin-EDTA (0.25%)

(GIBCO, 25200056) which it should be enough to cover the surface of the flask was added into the flask and cells inside trypsin were incubated (37 °C with 5% CO_2) for 5 min to remove the adherent cells from the flask surface. When the all cells were removed from the surface of flask, minimum the two volume of medium was added into the flask to inactivate the trypsin-EDTA. Suspended cells were transferred into a 15 ml falcon tube, centrifuged at 1600 rpm for 5 min and the supernatant was removed. Fresh medium replenished the tube. After mixing the cells and medium gently, 100 µl of cell suspension were resuspended in 200 µl of Trypan Blue (GIBCO, 15250061). The A hemocytometer was used to count the cells required 200 µl of 1X PBS solution to quantify the number of cells.

The cells were frozen in freezing medium composed of 10% DMSO (v/v) and 90% FBS (v/v). To freeze, cells were trypsinizied and centrifuged according to protocol above. After, supernatant was removed and an adequate volume of freezing medium was added into a falcon tube for resuspension of the cells to yield approximately 1-2 x 10^6 cells/ml. 1ml of cell suspension was transferred into cryotubes and placed into freezing container (Nalgene, 5100-0001) at -20 °C for 2 hours and stored -80 °C. For long term storage, vials were transferred to the liquid nitrogen tank.

3.6.2. Primary Cell Culture

3.6.2.1. Optimization of Cell Culture

Cells were isolated from the corneas obtained with the ethical approval. Optimization study was carried out by trying different media for cell isolation from tissue.

A 60 mm petri plate was coated with 0.2% gelatin (Sigma – Aldrich, G1890) before cell isolation from tissue. 0.02 mg gelatin dissolved in 10 ml warm PBS, which was vortexed to ensure complete dissolution. To ensure sterility, it was passed through 0.22 µm filters inside the laminar flow cabin. 2 ml sterile gelatin solution applied in petri plates and incubated (37 °C with 5% CO_2) for 2 hours. Before cell seeding, remaining excess gelatin solution inside the petri plate has been removed with the pipette.

Human cornea tissues from the hospital were placed in Optisol to preserve cell/tissue viability (Kureshi et al., 2014).

Corneal tissues were placed in 100 mm petri plate under aseptic conditions. Mechanical mincing was performed with the help of sterile forceps. For enzymatic digestion, 0.5 mg/ml type II collagenase (Sigma – Aldrich, collagenase from clostridium histolyticum, type II, C6885) was prepared in PBS and filter sterilized. Minced cornea tissue was digested in 0.5 ml of prepared type II collagenase solution in 8 ml of complete DMEM 10% FBS and incubated overnight.

After the digestion to remove excess collagenase solution cell-tissue slurry was centrifuged in the 15 ml falcon tube at 1600 rpm for 5 min and pelleted. Optimization of corneal cell isolation protocol was assessed in multiple trial with four different cornea tissues. After digestion isolated cell were resuspended and seeded using different culture medias such as Defined Keratinocyte Serum Free Medium (DKSFM) (GIBCO, 10744019), DMEM/F12 serum free (GIBCO, 31330-038), DMEM /F12 5% FBS and Complete DMEM 10% FBS and cultured in 60 mm gelatin coated petri plates. Depending on age of the donor adhesion and expansion of isolated corneal cells were observed in different time points varying between 6 to 15 days.

Table 4 Information about human cornea tissues.

Condition	Age	Gender
Macular Corneal Dystrophy Positive	20	M
Healthy	20	F
Macular Corneal Dystrophy Negative	70	F
Healthy	9	F

3.6.3. PMMA Mold Fabrication

To fabricate uniform size hydrogels, we first fabricated a mold from stiff polymeric material. A mold with a diameter of 2.5 cm and a depth of 3 mm which was designed by Corel Draw software. With the use of a laser cutter, the upper part was cut out of a 3 mm, and the lower part out of a 1.5 m thick Poly (methyl methacrylate) (PMMA) sheet. Double-sided tape was used to attach both. The hydrogels poured into the moldwere later cut out using 8 mm punches (Figure 8).

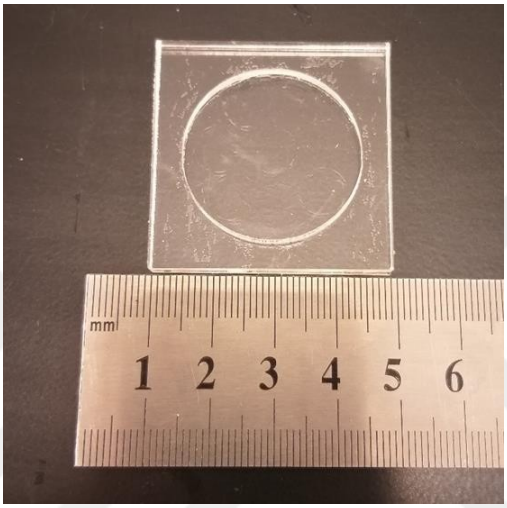

Figure 8 PMMA mold for the hydrogel preparation.

3.6.4. Hydrogel Synthesis

3.6.4.1. MES Buffer Solution Preparation

To prepare 0.625 M MES buffer, 1.3325 grams of 2-(N-Morpholino)ethanesulfonic acid (MES monohydrate) (Sigma – Aldrich, 69889) were dissolved in 10 ml dH_2O.

3.6.4.2. Gelatin Based Hydrogel

To produce gelatin based hydrogel, 0.2 g gelatin (Sigma – Aldrich, G2500) was dissolved in 2 ml of dH_2O, and MES buffer solution (600 µl) was added to gelatin mixture. Consecutively, 26.2 mg of NHS (Sigma – Aldrich, 130672) was dissolved in 100 µl of dH_2O in a different Eppendorf as a stock solution. 20 µl of stock NHS solution was mixed with the gelatin solution. For adjusting the pH of the solution to 5±0.5 0.1M Hydrochloric acid (HCl) (Sigma – Aldrich, 320331) was used (All solution were used at

room temperature). In a separate Eppendorf, 50 mg of MPC (Sigma – Aldrich, 730114) was dissolved in 400 µl of MES buffer solution by vortex. MPC and MES buffer solutions were mixed with 16.66 mg of PEGDA (Sigma – Aldrich, 455008, M_n 700) which dissolved in 400 µl of MES buffer. Following the preparation of all sub mixtures,they were collected in the same Eppendorf and mixed by pipetting.

In a separate Eppendorf tube, 40 mg of ammonium persulfate (APS) (Sigma – Aldrich, A3678) was dissolved in 1 ml of MES buffer solution. 40 µl of APS solution was added to the pre-prepared gelatin containing mixture. As a polymerization initiators N,N,N,Ntetramethylethylenediamine (TEMED) (Sigma – Aldrich, T9281) and EDC (Sigma – Aldrich, E7750) were used. 200 µl of TEMED were diluted with 800 µl of MES buffer solution, and 52 µl were quickly added to the gelatin containing mixture.In 100 µl of MES buffer solution, 43.7 mg of EDC was dissolved, and 40 µl of the EDCcontaining buffer solution was promptly added to the gelatin containing mixture and mixed by pipetting using 5 ml serological pipette.

The solution was combined with MPC in various ratios and made with various concentrations of gelatin using the same process, after which the 24-well plate was coated.

3.6.4.3. Collagen Type I from Bovine Tendon and MPC Hydrogel

Hybrid porous hydrogels composed of collagen and MPC were prepared as cell carriers. Here, previously reported hybrid hydrogel was adapted to the study with slight modifications (Islam et al., 2015). Lyophilized collagen type I was dissolved in 0.01 M HCl overnight. The collagen solution of 8 mg/ml density was diluted with 10x PBS (Gibco 70011036) to 6 mg/ml. The pH measurement was made with pH strips and the acidic solution was neutralized with the help of 1N Sodium hydroxide (NaOH). To prevent collagen foaming and to form homogenous solution, the mixture was prepared by pipetting. Different proportions of MPC, PEGDA were added (3:1 w:w). Thereafter, cross linkers EDC and NHS were added (1:1 mol:mol). 0. 66 mol 60 µl APS and 20 µl TEMED were added to solution. The final mixture was poured into PMMA molds and kept in a 37 °C water overnight for crosslinking. After crosslinking, hydrogels were cut

with an 8 mm diameter punch, and then to sterilize the hydrogels, they were transferred to 1% PS (Gibco,15140-122) containing PBS (PAN 36500).

3.6.5. Hydrogel Characterization

3.6.5.1. Electron Microscopy Analysis of Hydrogels

Porosity and morphology of prepared hydrogels were analyzed with SEM. Samples were prepared using modified published protocols (Sz & Ee, 2012). Briefly, the hydrogel samples were freeze-dried overnight in a lyophilizer (ThermoFisher). After lyophilization samples were coated 5 nm gold prior to imaging.

3.6.5.2. Electron Microscopy Analysis of Seeded Hydrogels

Cell-seeded hydrogels were analyzed by scanning electron microscopy on day 14 of static culture. Hydrogel without cells was used as a positive control. Sample preparation for SEM was performed by modifying published protocols (Sz & Ee, 2012). Briefly, hydrogel samples were fixed with 2.5% glutaraldehyde (Merck) in 0.1 M cacodylate buffer (Sigma – Aldrich, C0250) for 30 min. Without washing with another solution, it is taken into 7% sucrose and left for 15 min. This step is repeated one more time. It is kept in 2% Osmium tetroxide (OsO_4) (Cat. #19110) for 30 min without washing. Hydrogel samples are washed in distilled water for 5 min two times. Samples are dehydrated in increasing degrees of alcohol series (50%, 70%, 85%, 95%, 100%, 100%) for 5 min each step. Samples are kept in hexamethyldisilazane (HMDS) (Sigma – Aldrich, 440191) solution for 5 min. Later, the samples were dried overnight at room temperature. After the drying process, the samples were coated with 5 nm gold prior to imaging.

3.6.5.3. Mechanical Test

Three different samples were prepared for the mechanical test analysis of the developed hydrogels by mixing different collagen type I: MPC: PEGDA ratios. The samples were put through a compression test, which is appropriate for hydrogel structures of this size.

Each sample was taken out of the water at a specific moment and placed on the precision scale, where it was carefully taken with forceps and then weighed. This method was performed multiple times until each sample had a constant weight. The swelling percentages of hydrogels were calculated according to Equation 1 where Ws weight of swollen hydrogel and Wd is the hydrogel before immersion.

$$\text{Swelling}(\%) = \frac{Ws - Wi}{Wi} x100 \qquad (1)$$

3.6.6. Cell seeding and viability studies

The hydrogels were washed overnight at 4 °C in PBS containing 1% PS. Hydrogels were then seeded with $1x10^5$ 3T3 cells as well as isolated primary cells and incubated at 37 °C and 5% CO_2 for 7 days. After culture period, the hydrogels were rinsed three times with PBS and stained for 30 min at room temperature with Calcein AM solution (Biolegend, 425201). Cells were stained with Propidium Iodide (PI) (Biotium, 40017) solution (diluted with PBS 10:1 v/v) and incubated for 2 min at room temperature. Hydrogels were then observed under fluorescence microscope for cellular viability.

3.6.7. Disease Modeling and Verification

To develop the disease model, cells isolated from MCD negative patient cornea were used. The validation of the *in vitro* model were completed by the $NaClO_3$ (Sigma Aldrich, S3171) method developed by Murab et al. in 2016 (Murab et al., 2016). Different concentration of $NaClO_3$ were applied, and the optimum value was determined by qPCR and immunohistochemical staining. Presto Blue (Invitrogen by Thermo Fisher Scientific, A13261) staining was performed to observe the effect of $NaClO_3$ on cells. Samples were collected on days 1, 7, and 14 and performed Presto Blue assay according to the manufacturer's protocol. Briefly, added 1/10th volume of Presto Blue reagent directly to cells in culture medium and were incubated at 37 °C with 5% CO_2 up to 3 hours. Protected from sunlight during the procedure and absorbance values were taken inside the microplate reader at 570 nm, using 600 nm as a reference wavelength.

3.6.8. Gene expression profiles of primary cells

3.6.8.1. RNA Isolation

Experiments were conducted with cells that had not been exposed to $NaClO_3$ as the control group and cells that had been exposed to $NaClO_3$ at doses of 5mM, 10mM, 25mM, and 50mM as the test group. On day 7, the cultured cells were placed in TRIzol (TRI Reagent by Molecular Research Center, T 118). An RNA isolation kit was used to isolate the RNA (Macherey-Nagel, 740955.50). After freezing the lysates on ice, they were incubated at room temperature for 5 min. Chloroform was added as 20% ofthe volume of TRIzol. It was incubated for 2 min at room temperature after homogeneitywas accomplished by gently tossing it up and down. To achieve phase separation, it was centrifuged at 12000 rpm for 15 min at 4 °C. The RNA-containing supernatant was collected. 70% ethanol by volume of the collected liquid phase was added and incubated for 10 min at room temperature. RNA isolation from the lysate/ethanol mixture was then performed in accordance with the kit protocol. The amount and purity of RNA were measured with the NanoDrop device.

3.6.8.2. cDNA Synthesis and qPCR Analysis

The cDNA synthesis from the obtained RNAs was carried out using the ABM OneScript Plus cDNA Synthesis Kit (G236).

Analysis of cDNAs obtained from cells with and without $NaClO_3$ treatment was carried out with GoTaq Master Mix (Promega, A6002) on an Applied Biosystem 7500 Fast Realtime PCR device for relevant genes. Results evaluated using Prism8 and Excel.

Table 5 qPCR Protocol

Stages	Number of Cycles	Temprature (˚C)	Time (second)
Holding	1	95	120
Cycling	40	95	10
		60	10
		72	30
		95	15
Melt Curve	1	60	60
		95	15
		4	∞

Table 6 Primer list for qPCR

Primer	Forward	Reverse
MMP1	5-GCATATCGATGCTGCTCTTTC-3	5-GATAACCTGGATCCATAGATCGTT-3
MMP13	5-CCAGAACTTC CCAACCAT-3	5-ACCCTCCATAAT GTCATACC-3
MMP2	5-CCCCAAAACGGACAAAGAG-3	5-CTTCAGCACAAACAGGTTGC-3
COL1A1	5- GGGATTCCCTGGACCTAAAG-3	5- GGAACACCTCGCTCTCCA -3
FN1	5-GCGAGAGTGCCCCTACTACA-3	5-GTTGGTGAATCGCAGGTCA-3
CHST6	5- TCATCTCCCATGGATTTGTG-3	5- GCCACATGCTGACTGCTG -3
ALDH1A1	5- CATTGGCACCTGGAACTACC-3	5- GGCTTGAGGACCACTGAGTT-3
ALDH3A1	5- GCTGTTGAATTTGCACACC-3	5-CCCCTTCTTTCTTCCCACTC-3

3.6.9. Immunofluorescence Assay

Primary cells isolated from the metabolically healthy but scarred patient and $NaClO_3$ treated groups were seeded in a 48-well plate. The list of primer antibodies and seconder antibodies used is given in Table 7 and Table 8. The cell seeding densityis $5.4x10^4$ cells / cm^2. At the end of 7 days, it was fixed with 4% paraformaldehyde (PFA) for 30 min at room temperature, and then washed with PBS and stored at +4 °C. After fixation, cells were permabilized with 0.3% Triton X-100 and then blocked with PBS containing 1% bovine serum albumin (BSA) / 0.05% Tween-20 at room

temperature for 1 hour. After blocking, antibodies were diluted in special blocking buffer and incubated overnight at +4 °C. The next day, washing was done with 3x PBS-T for 5 min. Anti-rabbit AF-488 (Jackson Immuno, 711-545-152) and Anti-mouse secondary antibodies were diluted 1:800 and incubated for 2 hours in the dark at room temperature. Washing was done with 3x PBS-T for 5 min. 1 µg/ml DAPI (neoFroxx) was added and incubated for 10 min in the dark at room temperature. After washing with 3x PBS for 5 min each, they were visualized with PBS using a fluorescent microscope (Olympus IX71).

Table 7 Primer Antibody list for immunofluorescence

Primer Antibody	Source	Brand/Catalog Number	Incubation Concentration
Anti MMP1	Rb	Abcam / ab137332	1:200
Anti MMP13	M	SantaCruz/sc515284	1:200
Anti LUM	M	SantaCruz/sc166871	1:200
Anti DEC	Rb	Abcam / ab175404	1:500
Anti Collagen I	Rb	Abcam / ab34710	1:200
Anti Collagen VI	Rb	Abcam / ab6588	1:500
TIMP 1	M	SantaCruz / sc-365905	1:100
TIMP 2	Rb	Abcam / ab-180630 - R	1:500
Mimecan	M	SantaCruz / sc-374463	1:100

Table 8 Seconder antibody is for immunofluorescence

Seconder Antibody	Source	Brand/Catalog Number	Incubation Concentration
Anti-Rabbit Ig H&L, 555	Rabbit	Cell Signaling / 4413S	1:1000
Anti-Mouse Ig H&L, 488	Mouse	Cell Signaling / 4408S	1:1000

3.6.10. Microfluidic Platform Design

Microfluidic platform molds were fabricated using rectangle PMMA sheets with 3 mm height. The microfluidic platform was designed with SolidWorks and COMSOL software and the molds were cut using a laser cutter (Epilog MINI, Epilog, USA) (Figure 9).

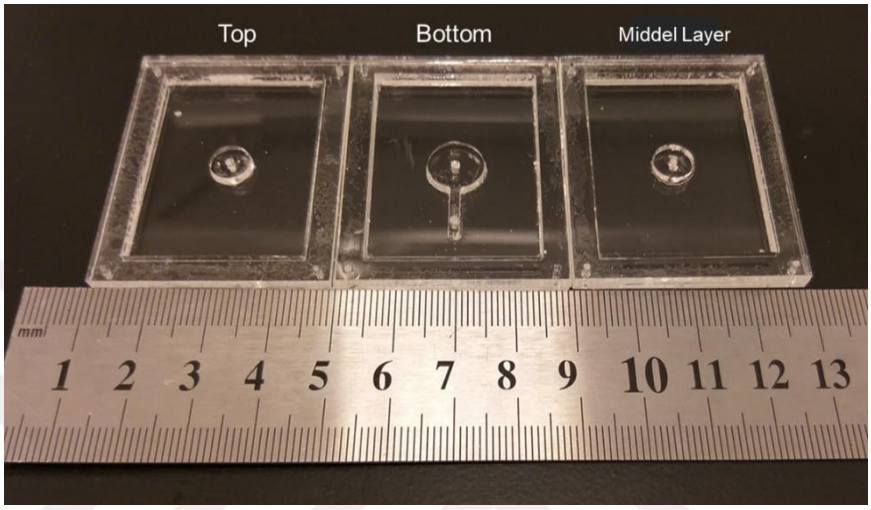

Figure 9 PMMA mold designs for microfluidic chips

The PDMS solution was made using Sylgard 184 Silicone Elastomer Kit. The PDMS base solution was combined with the crosslinker in a 10:1 (w/w) and poured into PMMA molds. For preventing bubble formation, the remaining air in the solution was removed with vacuum. PDMS was polymerized in an oven at 80 °C for up to 3 hours.

3.6.11. Cell seeded hydrogels

For seeding the primary cells on the hydrogel, firstly, medium was removed from 60 mm cell culture plate and cells were gently washed with 1X PBS to remove left over medium inside the flask. Then, 1 ml trypsin-EDTA (0.25%) (Gibco, 25200056) which was enough to cover the surface of the flask was added into the flask and cells inside trypsin were incubated (37 °C with 5% CO_2) for 3 min to remove the adherent cells from the flask surface. When the all cells were removed from the surface of flask, minimum the two volume of medium was added into the flask to inactivate the trypsin-

EDTA. Suspended cells were transferred into a 15 ml falcon tube, centrifuged at 1600 rpm for 5 min and the supernatant was removed. Fresh medium replenished the tube. After mixing the cells and medium gently, 100 µl of cell suspension were resuspended in 200 µl of Trypan Blue). The hemocytometer was used to count the cells required 200 µl of 1X PBS solution to quantify the number of cells.

Cell seeding was made approximately $3.0x10^4$ cells/hydrogel. After a week of culture of cells on hydrogel the constructs were placed into microfluidic platforms.

3.6.12. Histology

Cell seeded hydrogels were fixed overnight with 4% PFA at +4 °C after the end of the culture period inside the microfluidic platform. After fixation, samples were washed three times with 1X PBS and transferred in 30% sucrose (Merck, 1.07651.1000) and stored at +4 °C. The cell seeded hydrogel samples that had sunk to the bottom of the container were transferred to a separate container and frozen in liquid nitrogen with OCT (Tissue Tek) embedding material. A cryostat was used to take 8 µm frozen sections (Leica, CM1950).

Immunofluorescent stainings characterizing the phenotype of cells were performed same method as described above (3.6.11. Immunofluorescence Assay).

3.6.13. Alternative Treatment Methods Trails

As an alternative treatment, enzyme replacement therapy has been tried. The Kalyoncu laboratory team generated recombinant MMP1 and MMP13 enzymes as part of the TUBITAK (318S208) project. The model was used to evaluate enzymes whose activity had been determined by Kalyoncu Lab.

Different rates of enzyme were given to the primary cells and viability analyses were performed before the enzyme dose was determined. The enzyme was diluted from the stock solution and put to a 96-well plate in the following ratios, followed by plate analyses with Presto Blue solution (Concentration of MMP1 was 0.2 mg/ml and Concentration of MMP13 was 0.15 mg/ml). All the enzymes used in the experiment were diluted from the main stock with the concentration of 2000 ng/ml stock (Table 9 and Table 10). The Presto Blue solution was applied as directed by the manufacturer.

The cell media was collected with a pipette after 24 and 48 hours of enzyme application. The cells were then treated with 10 µl of presto blue solution and 90 µl of DMEM (High Glucose) (Phenol and FBS-free) medium in the incubator for three hours. The results were read in a plate reader and analyzed with Excel after incubation.

Table 9 MMP1 Concentration and Cell Culture Media Ratios

	Concentration	MMP-1 2000ng/ml	Cell Culture Media
24h	2000 ng/ml	100 ul	0 ul
	1500 ng/ml	75 ul	25 ul
	1000 ng /ml	50 ul	50 ul
	750 ng/ml	37.5 ul	62.5 ul
	500 ng/ml	25 ul	75 ul
	250 ng/ml	12.5 ul	87.5 ul
	50n g/ml	2.5 ul	97.5 ul
	0 ng/ml	0 ul	100 ul
	Concentration	**MMP-1 2000ng/ml**	**Cell Culture Media**
48h	2000 ng/ml	100 ul	0 ul
	1500 ng/ml	75 ul	25 ul
	1000 ng /ml	50 ul	50 ul
	750 ng/ml	37.5 ul	62.5 ul
	500 ng/ml	25 ul	75 ul
	250 ng/ml	12.5 ul	87.5 ul
	50n g/ml	2.5 ul	97.5 ul
	0 ng/ml	0 ul	100 ul

Table 10 MMP13 Concentration and Cell Culture Media Ratios

	Concentration	MMP-13 2000ng/ml	Cell Culture Media
24h	2000 ng/ml	100 ul	0 ul
	1500 ng/ml	75 ul	25 ul
	1000 ng /ml	50 ul	50 ul
	750 ng/ml	37.5 ul	62.5 ul
	500 ng/ml	25 ul	75 ul
	250 ng/ml	12.5 ul	87.5 ul
	50n g/ml	2.5 ul	97.5 ul
	0 ng/ml	0 ul	100 ul
	Concentration	**MMP-13 2000ng/ml**	**Cell Culture Media**
48h	2000 ng/ml	100 ul	0 ul
	1500 ng/ml	75 ul	25 ul
	1000 ng /ml	50 ul	50 ul
	750 ng/ml	37.5 ul	62.5 ul
	500 ng/ml	25 ul	75 ul
	250 ng/ml	12.5 ul	87.5 ul
	50n g/ml	2.5 ul	97.5 ul
	0 ng/ml	0 ul	100 ul

After the viability tests, the cells were given the three selected concentrations for 48 hours, and qPCR analyses of the samples were performed same method as described above (3.6.8. Gene expression profiles of primary cells).

3.7. Research Plan

Research plan of the thesis is given in the table below.

Table 11 Research plan of the thesis

	March 2020 – Dec. 2020	Dec. 2020 – Jan. 2022	Jan. 2022 – May 2022
Literature Review	X	X	
Planning the Experiments	X	X	
Data Collection and Experiments		X	X
Evaluation of data		X	X
Thesis Writing			X

3.8. Evaluation of Data

In this thesis GraphPad Prism 8 and Microsoft Excel were used to analyze the qPCR data. Immunocytochemistry (ICC) and immunohistochemistry (IHC) images were analyzed with ImageJ and Zen 3.1 (Blue edition) softwares.

3.9. Limitation of Research

Primary cell isolation from tissue was carried out in this research. In this context, variations in cell proliferation and adhesion were detected in donor tissues depending on disease, age, and gender.

The COVID-19 pandemic caused some difficulties during the research. The duration of the trial was extended by stopping the surgeries in hospitals for a while.

3.10. Ethics Committee Approval

This thesis was approved by Ethics Committee of IBG-GOEK with the protocol number “2021-004”.

The human corneas were used after taking the Patient Consent Forms.

Approval from the Ethics Committee and an example of a Patient Consent Form were included in the Appendix section.

4. RESULTS

4.1. Primary Cell Culture Optimization

Optimization trials for several mediums were carried out to culture primary cells derived from either healthy or diseased corneas. Four different culture media formulations were tested for their impact on cell growth and adherence. Even after one week, no cell attachment was seen in three different culture media formulations (Figure 10). Only upon culture with DMEM supplemented with 10% FBS and 1% P/S isolated primary cells (both from MCD (+) and (-) patients) adhered and start to proliferate in average of 5 days and reached confluency approximately in 20 days (Figure 11).

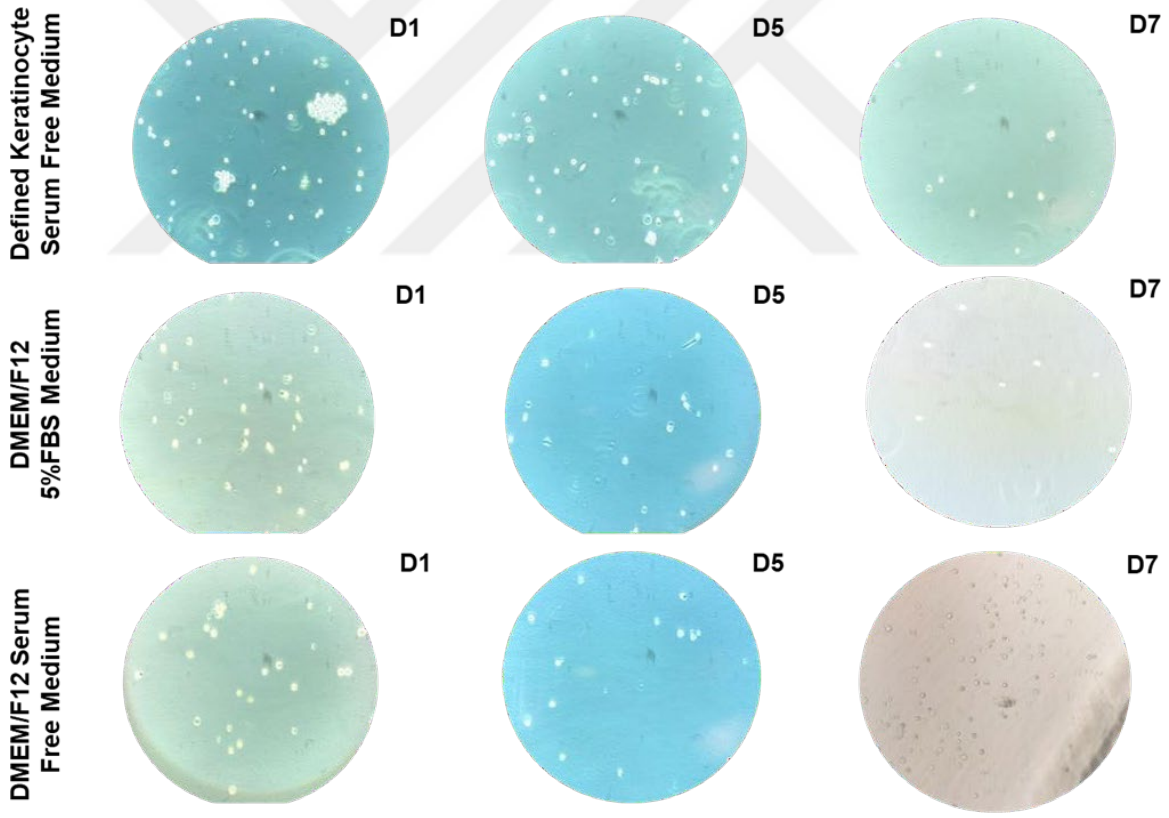

Figure 10 Three alternative mediums were evaluated for one week during the optimization experiments. None of the formulations supported the cell adhesion and proliferation.

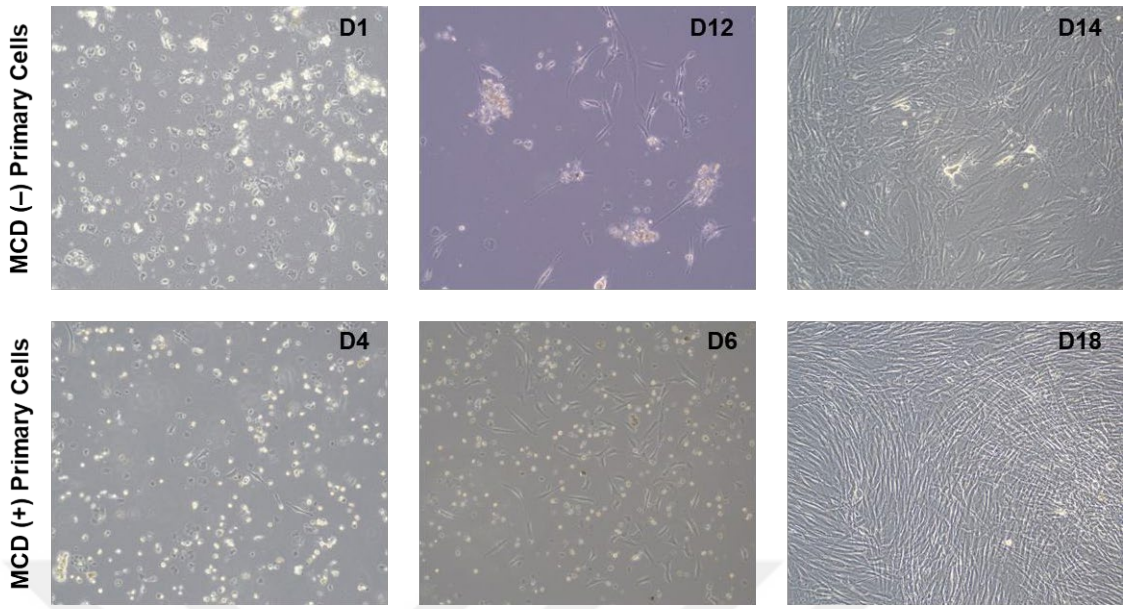

Figure 11 Bright field images of primary cells isolated from MCD (+) and MCD (-) patients at different culture periods.

Primary corneal cells were checked for preservation of phenotype at day 7. Expression of corneal stromal cell markers, lumican, Timp2, keratocan, collagen VI and collagen I were detected with ICC (Figure 12A and D), indicating that cells maintained their characteristic phenotype properties during the culture period.

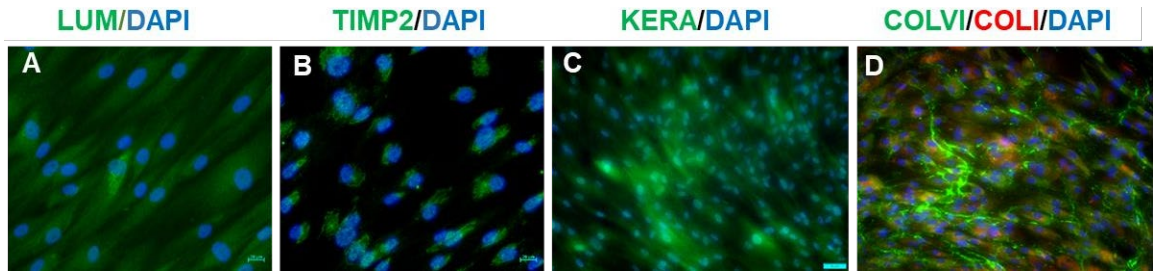

Figure 12 Isolated primary cells stained against A) ECM protein marker Lumican (LUM) B) cornea remodeling marker TIMP2 C) Corneal transparency marker keratocan and D) ECM marker Collagen I and Collagen VI. Nuclei are stained with DAPI.

4.2. Gelatin Based Hydrogel

Gelatin based hydrogels containing MPC, PEGDA were developed as cell carriers. First hydrogels were optimized for composition/ratio of polymers and crosslinking parameters. Generated hydrogels were evaluated for physical properties such as optical clearance, gelation, mechanical strength, and handling. Further the biocompatibility of the crosslinking process and obtained hydrogels was assessed. All hydrogels generated using different ratios of MPC and gelatin were optically transparent (Figure 13). The surface properties of porcine skin hydrogels produced in various ratios were examined by using SEM imaging. In SEM micrographs, homogeneity of the surface hydrogel pore sizes and their distribution was observed. With the fixed concentration of gelatin (10%) increased ratio of gelatin solution (Gelatin: MPC 2:1, Gelatin: MPC 4:2) increases the porosity of the surface as shown in Figure 14A and Figure 14B. We observed that, due to low pore size and surface structure of 13% gelatin concentration in Figure 14C, 14D and 14E is not suitable for penetration of culture media through the hydrogels. When the gelatin concentration increased to 15%, quality of surface porosities has significantly increased as well. Especially, in Gelatin: MPC 2:1 (w:w) ratio shows more regular pore structures as it seen in Figure 14F, 14G and 14H. Also, the data shows that, 15% of gelatin concentration hydrogels result with better porosity compared to 18% and 20% of gelatin. However, only 18% gelatin concentration results in porous structures but still, it wasn't close to expected pattern quality comparing with 13% and 15% concentrations (Figure 14I – M).

Determining the hydrogel concentration for further use in the study was made according to SEM micrograph evaluations. 10% Gelatin: MPC 4:1 (w:w) and 15% Gelatin: MPC 2:1 (w:w) concentration ratios have been selected due to their homogeneous porous structure.

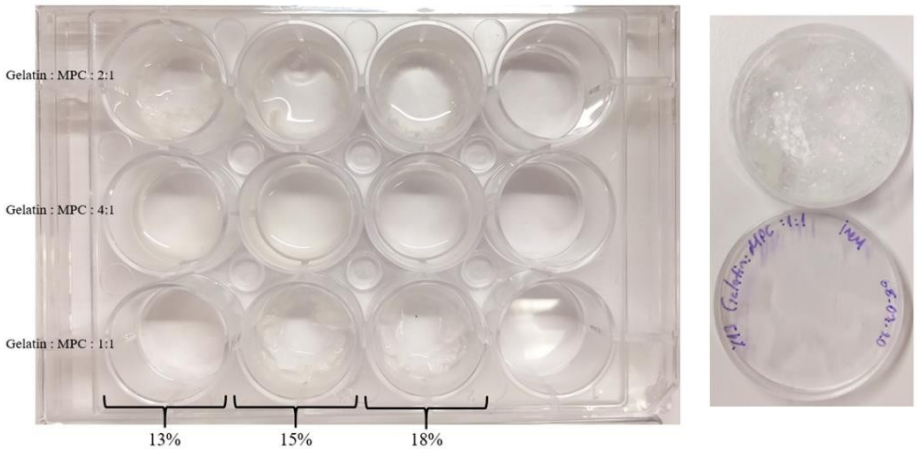

Figure 13 Transparency of gelatin based hydrogels with different concentrations of gelatin.

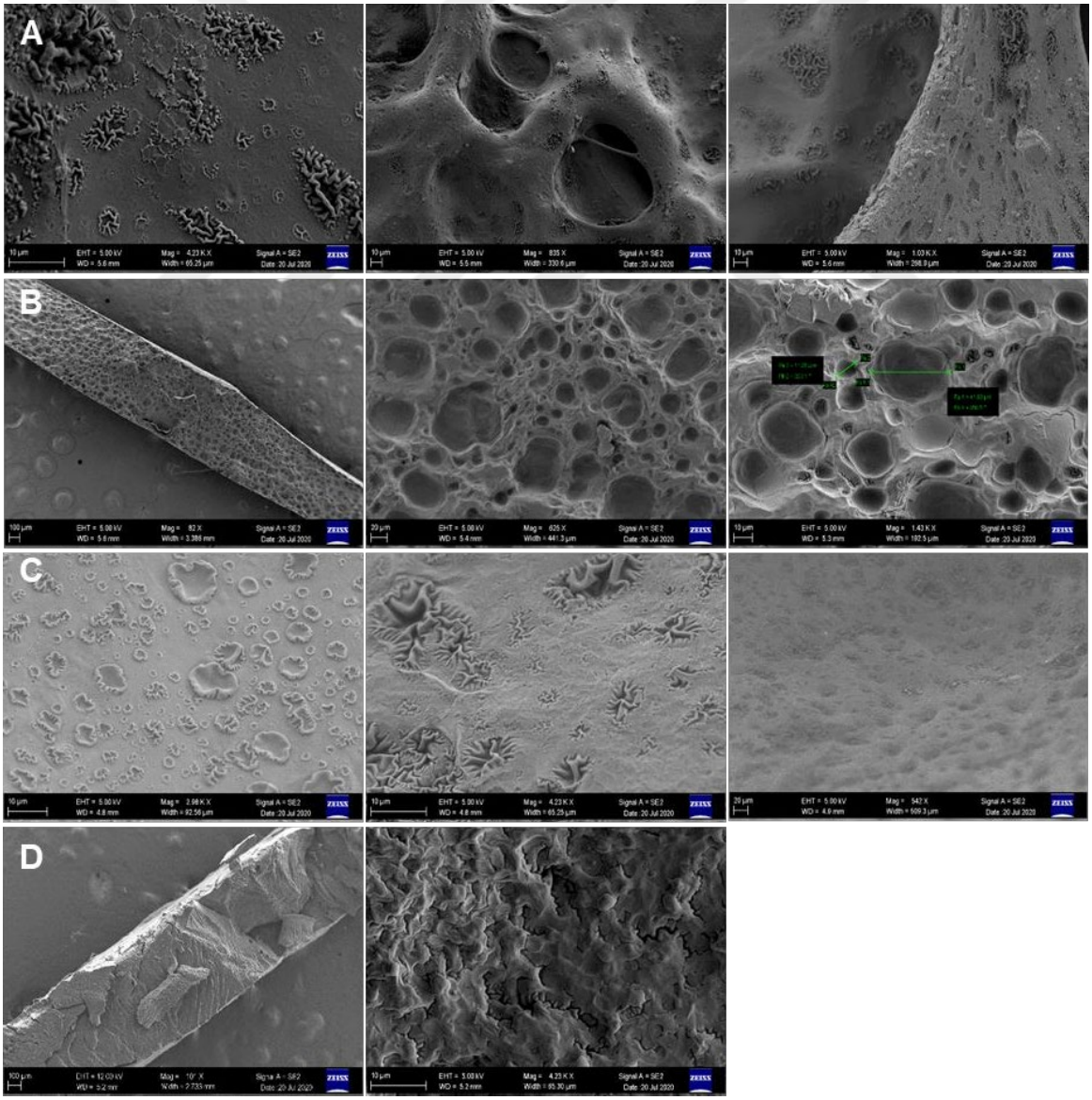

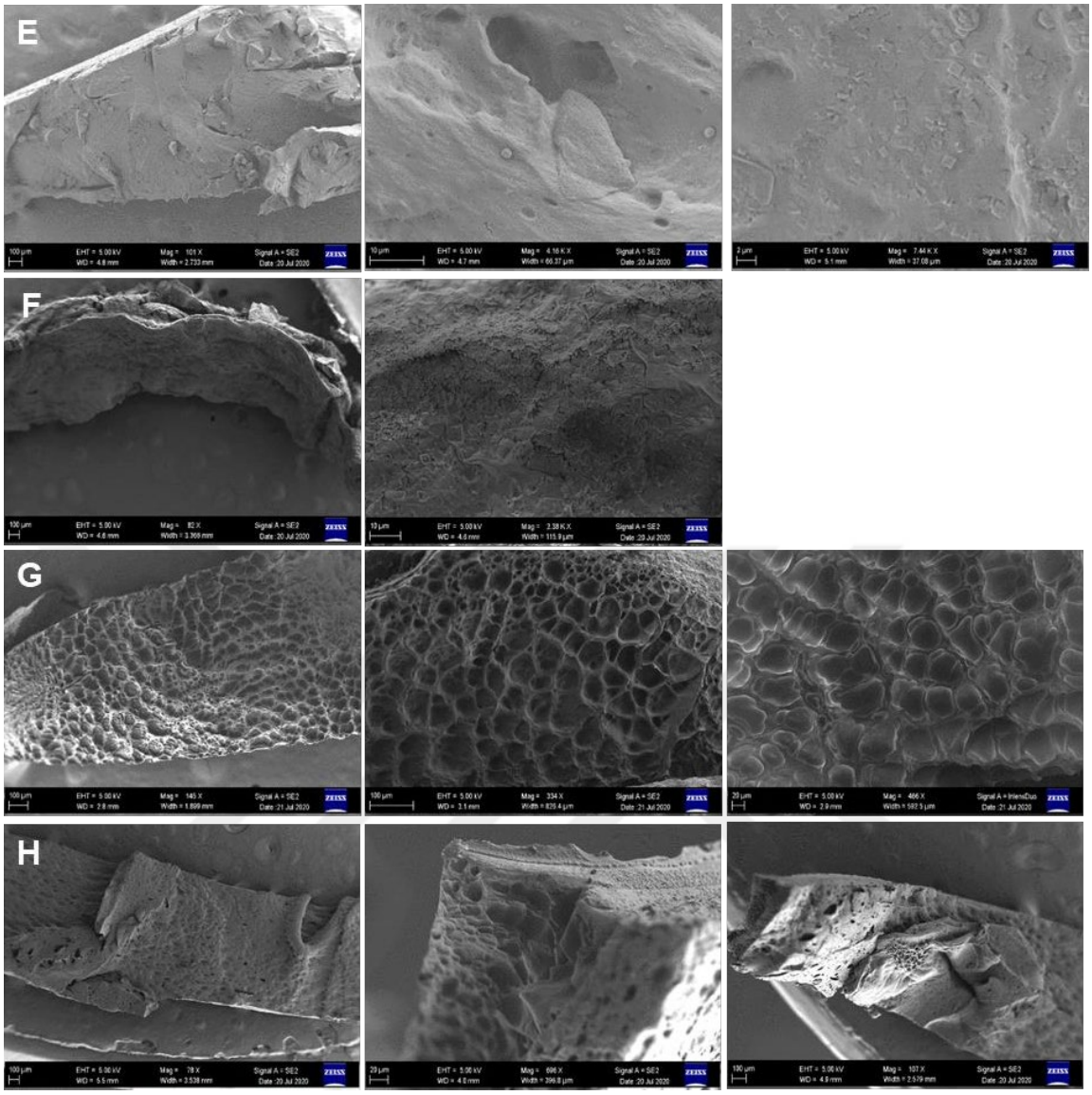
E
F
G
H

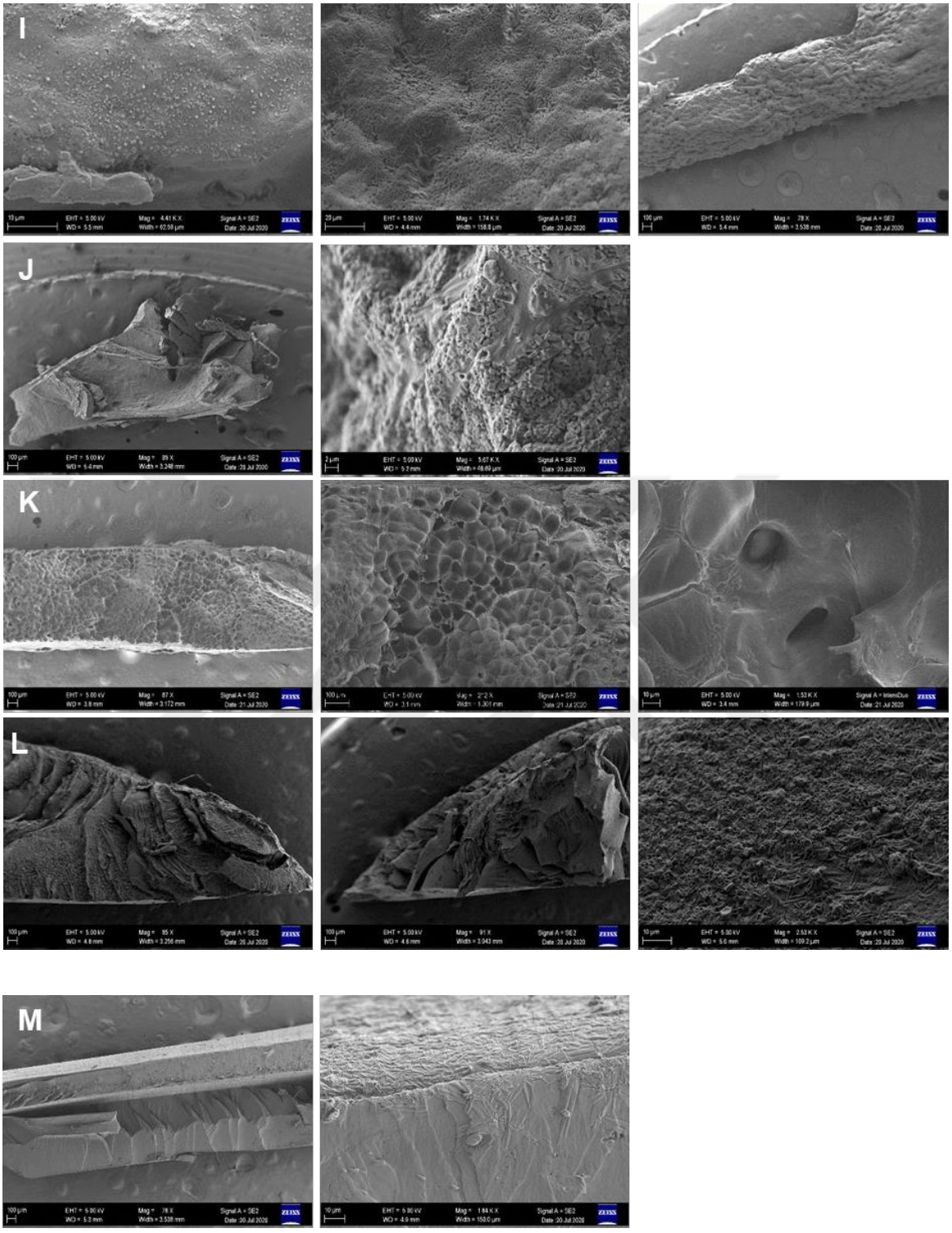

Figure 14 Electron microscopy images of gelatin-based hydrogels. A) 10% Gelatin : MPC : 2:1 B) 10% Gelatin : MPC : 4:1 C) 13% Gelatin : MPC : 1:1 D) 13% Gelatin : MPC : 2:1 E) 13% Gelatin : MPC 4:1 F) 15% Gelatin : MPC 1:1 G) 15% Gelatin : MPC : 2:1 H) 15% Gelatin : MPC : 4:1 I) 18% Gelatin : MPC 1:1 J) 18% Gelatin : MPC 2:1 K) 18% Gelatin : MPC 4:1 L) 20% Gelatin : MPC : 2:1 M) 20% Gelatin : MPC : 4:1

Chosen hydrogels, were tested for their ability to cross-link both under nitrogen at and nitrogen-free environment at room temperatures, based on the method described in the literature (Islam et al., 2015). The yellow colors of the phenols in the Figure 15 indicates the negative impact on the cell viability of nitrogen-free environment. A Calcein/PI staining results clearly shows, viable cell on both 10% and 15% of gelatin concentrations as in Figure 16. Which proves that gelatin concentrationdoes not affect cell viability.

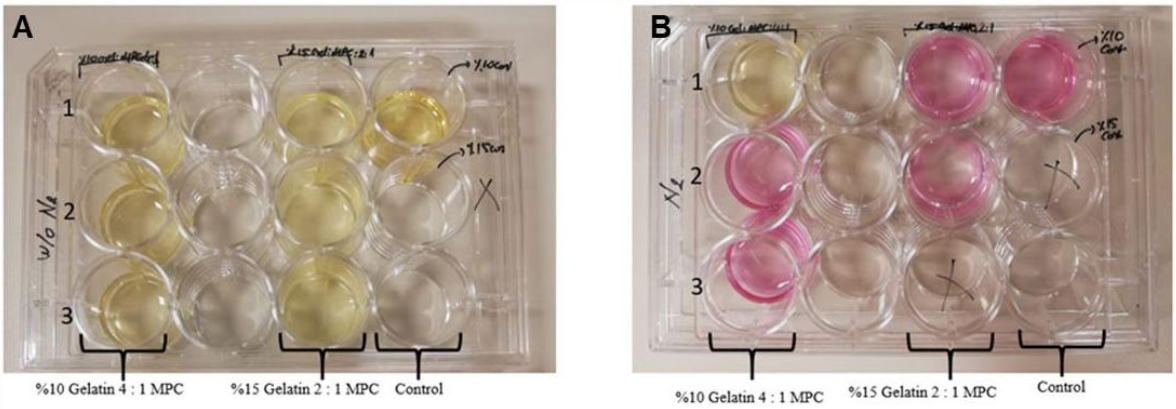

Figure 15 24h later after 3T3 cell seeding A) Under nitrogen - free environment and B) Under nitrogen

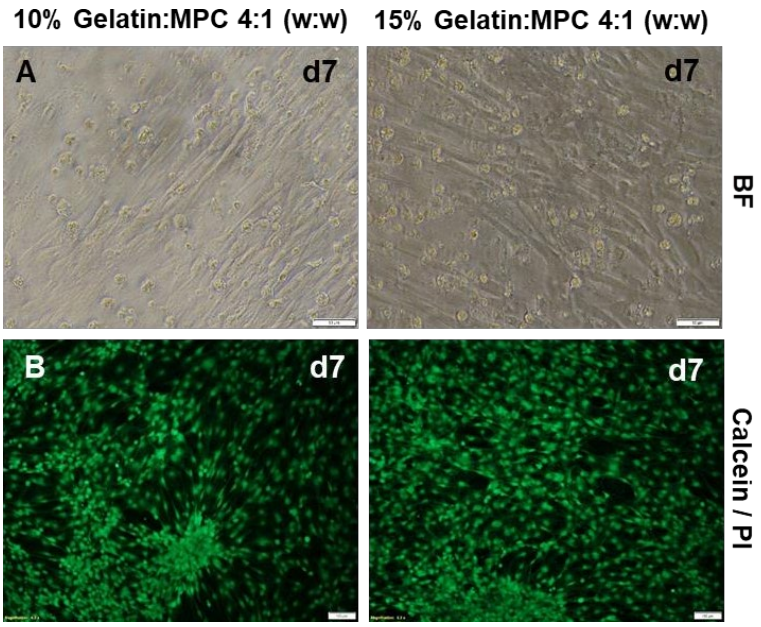

Figure 16 Cell seeding on the hydrogel after crosslinking under nitrogen A) Bright Field (BF) imaging and B) Calcein/PI imaging

4.3. Collagen Type I Based Hydrogel

After literature research, hydrogels made from collagen type I shows better cross-linking in a water bath with the effect of humidity instead of nitrogen (Figure 17) (W. Liu et al., 2008). 3T3 cells were seeded at a density of $2x10^4$ cells/gel. Calcein/PI staining results shows that, the crosslinking in humid environment does not have negative effect on cell viability (Figure 18 and Figure 19).

Figure 17 Synthesized Collagen:MPC:PEGDA (7.5:1:1.5) hydrogel from the side and front view

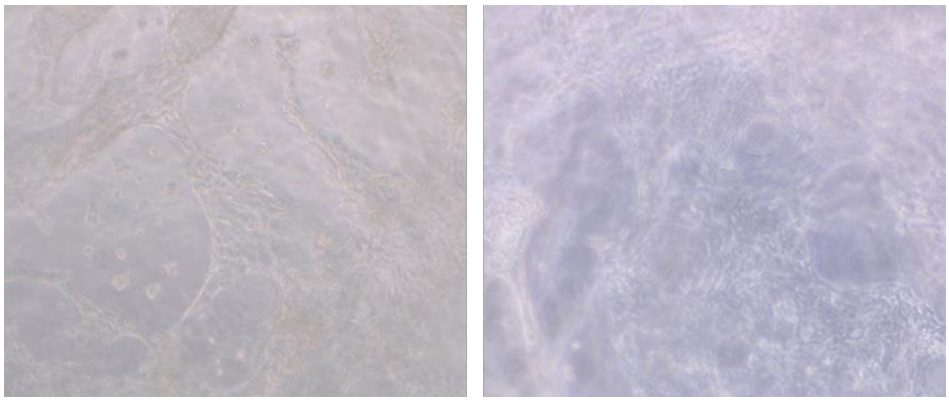

Figure 18 3T3 cell seeded collagen type I : MPC : PEGDA 7.5:1:1.5 (w:w) hydrogel.

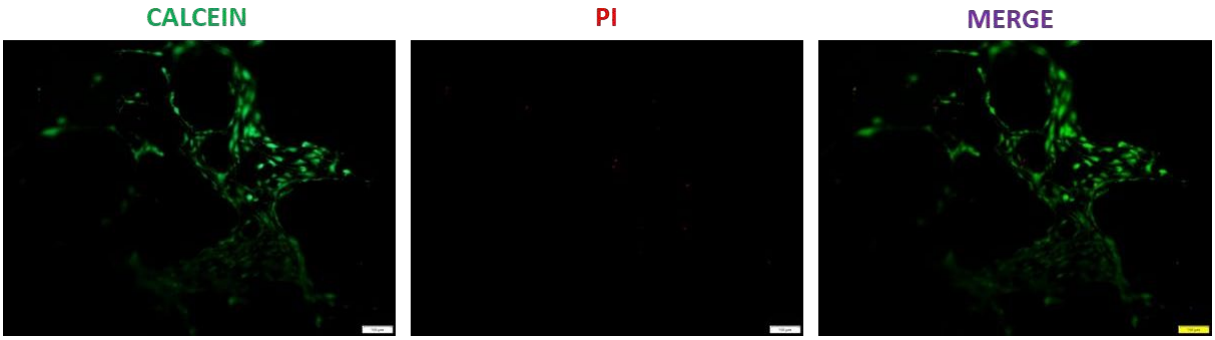

Figure 19 Calcein/PI stainings of 3T3 cell culture on collagen type I : MPC : PEGDA 7.5:1:1.5 (w:w) hydrogel.

After the cell viability was confirmed, primary corneal stromal cells, which are more sensitive compared to 3T3 cells were seeded on the hydrogel. Corneal stromal cells maintained their fibroblastic morphology as seen in the Bright Field Microscopy (BF) (Figure 20). Also their viability has been assessed by Calcein/PI staining (Figure 21).

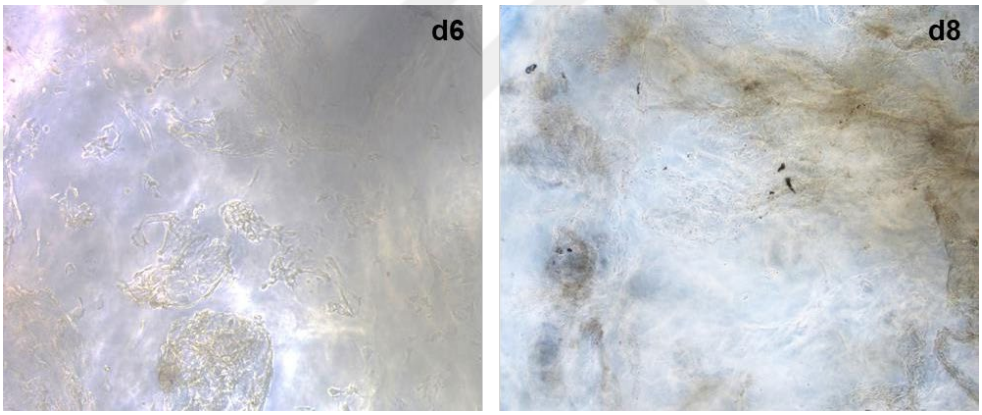

Figure 20 Collagen type I : MPC :PEGDA 7.5:1:1.5 (w:w) hydrogel with primary cells.

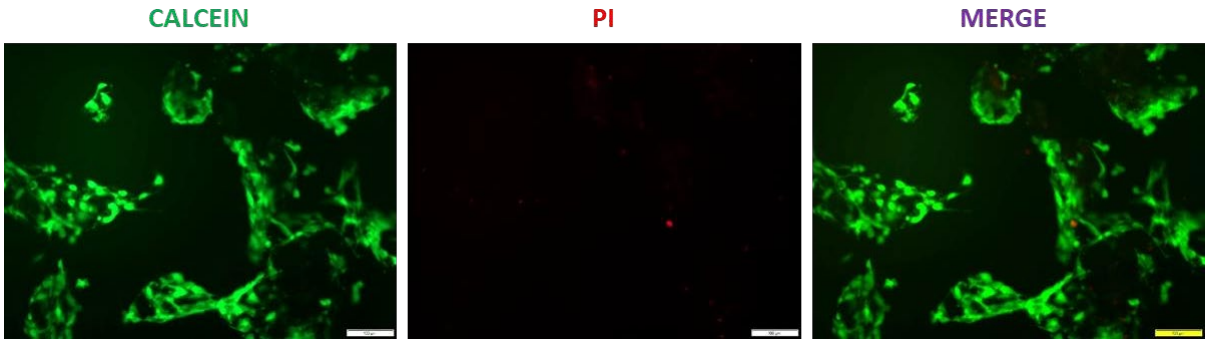

Figure 21 Collagen type I : MPC :PEGDA 7.5:1:1.5 (w:w) hydrogel with primary cells on day14 and Calcein/PI stainings.

The mechanical test and swelling ratio analysis of the developed hydrogel were carried out for three different collagen ratios (Collagen:MPC:PEG 7.5:1.1.5, Collagen:MPC:PEG 4:1:1.5 and Collagen:MPC:PEG 2:1:1.5). These results were compared with each other. Based on their water absorption capacity, swelling ratio analysis was performed on the hydrogels. The water holding capacity was calculated as a percentage using the weight difference ratio between day-four and day-one as described in the methods section. When created hydrogel contains a large amount of crosslinker which effects porous structure of hydrogel, it could be characterized by low water holding capacity. A significantly more compact hydrogel with smaller mesh sizes are associated with low water holding capacity which means low cross linker density (Kowalski et al., 2019). When comparing the results, we discovered that the selected hydrogel had a lower water holding capacity and a smaller mesh size, which allowed us to manipulate it more easily for further experiments (Figure 22A). The compression test was used to determine the mechanical properties of hydrogels as the collagen concentration increased, the hydrogels became stiffer (Figure 22B).

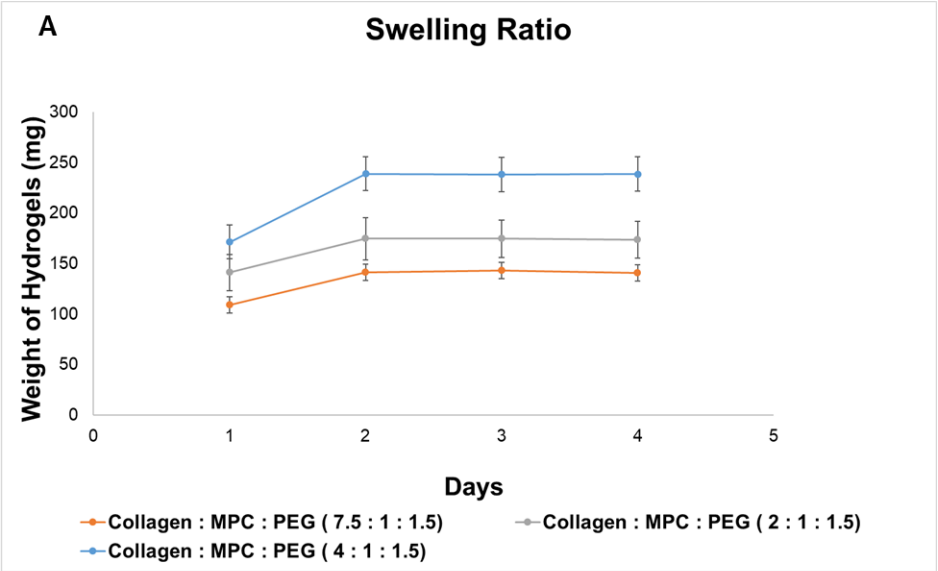

(w:w)	(%) Swelling Ratio
Collagen : MPC : PEG (7.5 : 1 : 1.5)	28,948
Collagen : MPC : PEG (2 : 1 : 1.5)	22,957
Collagen : MPC : PEG (4 : 1 : 1.5)	39,269

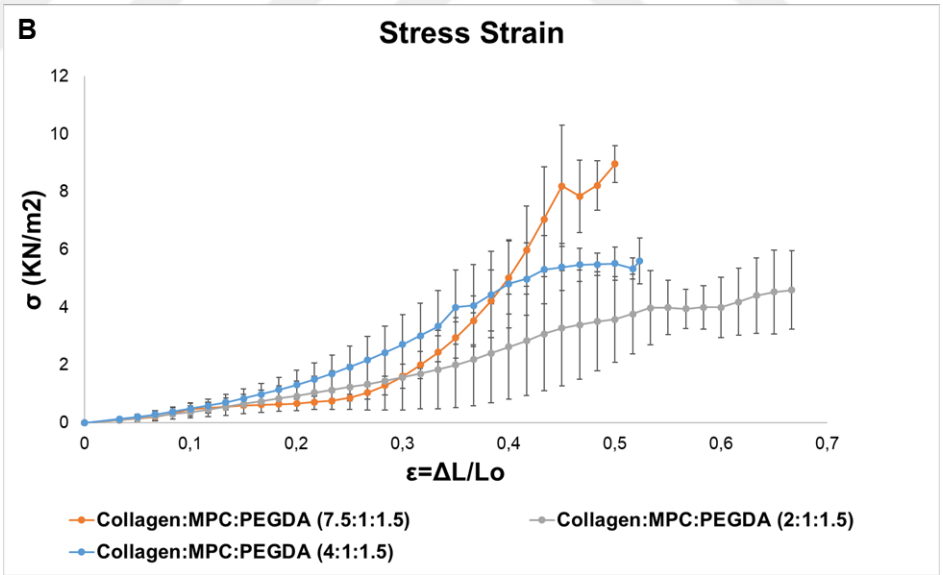

Figure 22 Stress-strain and swelling ratio analyzes of 3 different hydrogels A) Swelling ratio results B) Stress-strain diagram.

Following the mechanical analysis of the hydrogels, different ratio of Collagen I: MPC (Collagen type I : MPC : PEGDA (2:1:1.5)), (Collagen type I : MPC : PEGDA (4:1:1.5)), (Collagen type I : MPC : PEGDA (7.5:1:1.5)) were subjected to SEM

analysis. In addition, the hydrogel selected for future experiments (Collagen type I : MPC : PEGDA (7.5:1:1.5) was subjected to cell and cell-free SEM analyses. According to the SEM analysis, the presence of collagen fibrils became more noticeable when the ratio of collagen is increased. More viable cells were observed as a result of increased collagen concentration (Figure 23).

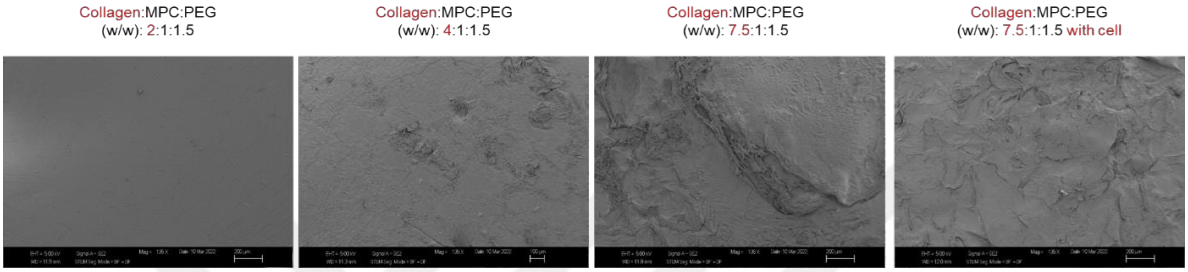

Figure 23 SEM analysis of hydrogel samples of various ratios.

4.4. Disease Modeling and Validation

$NaClO_3$ was used at various concentrations to simulate macular corneal dystrophy (Murab et al., 2016). Presto blue viability analysis was used to determine whether $NaClO_3$ had a toxic effect on cells before determining the appropriate dose. At higher concentrations and long culture period, no negative effects were seen on cell viability (Figure 24).

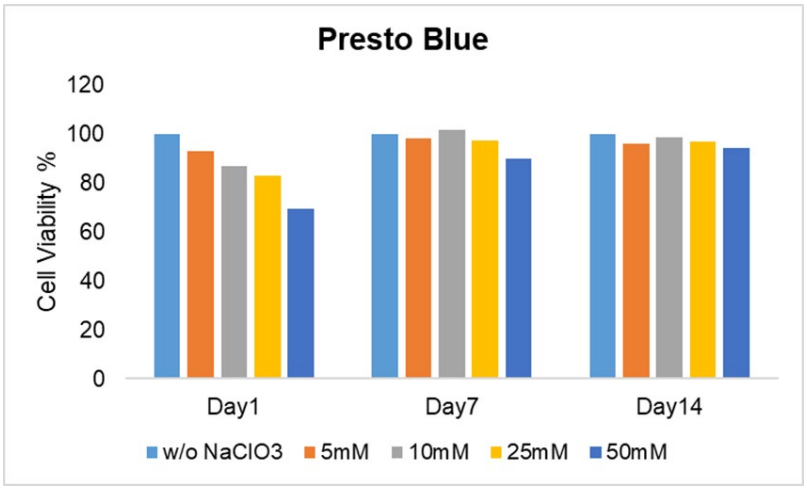

Figure 24 Effect of a 14-day treatment of $NaClO_3$ on cell viability.

To identify the proper $NaClO_3$ concentration and application period to use for disease modeling, immunofluorescent staining of primary corneal stromal cells and their MMP1, MMP13, MMP2, Fibronectin 1, COL1A1, CHST6, ALDH1A1 and ALDH3A1 genes expression in mRNA levels were analyzed. Fluorescence intensity analysis was performed and color intensities converted int numeric values via ImageJ. During the course of the disease, low MMP1 and MMP13 expression levels were observed. $NaClO_3$ appears to induce MCD (-) cells to behave like MCD (+) cells as the culture time increases in the disease model. Following fluorescence intensity analysis, we report that, length of culture period and concentration reduces the expression of MMP1, MMP13, and increased collagen I levels in injury model (Figure 25).

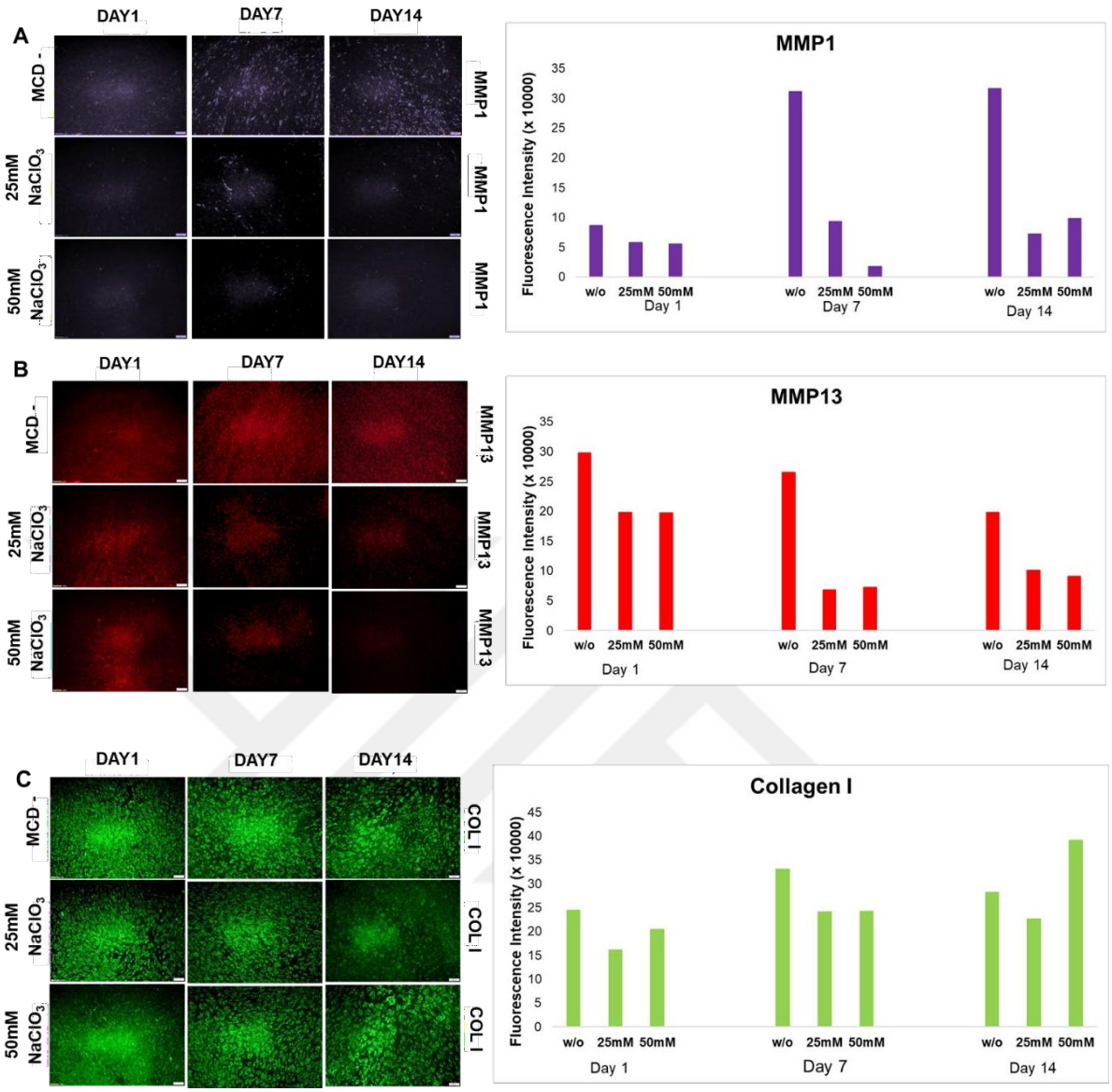

Figure 25 Isolated primary cells from MCD (-) patient and treated with different concentration of $NaClO_3$ stained against A) matrix metalloproteinase -1 (MMP1) B) matrix metalloproteinase 13 (MMP13) and C) extracellular matrix protein marker Collagen I. Intensity analysis were done with ImageJ.

The same strategy was followed to stain cells obtained from MCD (+) patients, and the intensities were measured by ImageJ. As a result of the fluorescence intensity measurement on the MCD (+) cells, level of decrease is comparable to $NaClO_3$ model particularly on day 7 (Figure 26).

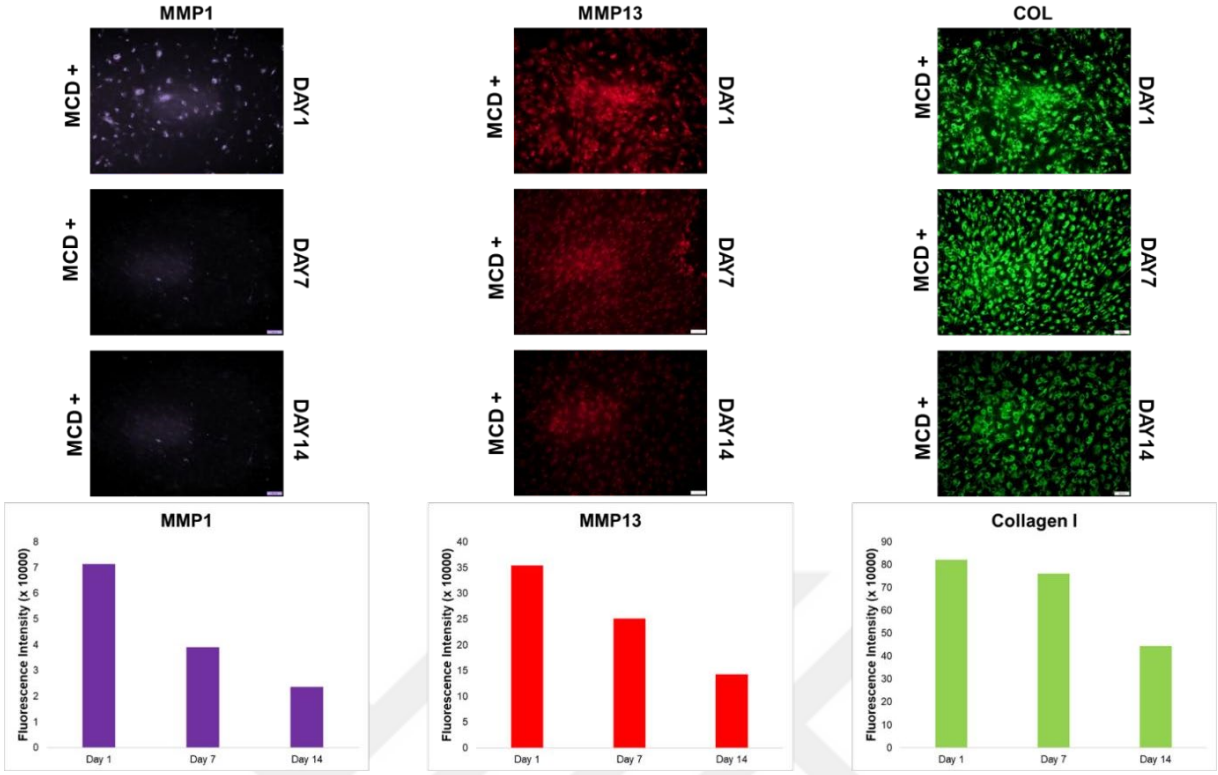

Figure 26 Isolated primary cells from MCD (+) patient stained against matrix metalloproteinase markers (MMP1 and MMP13) and extracellular matrix protein marker Collagen I. Intensity analysis were done with ImageJ.

According to these results, 7-day culture period used for the qPCR analysis for the identify the optimal dose of $NaClO_3$. 50mM $NaClO_3$, 25mM $NaClO_3$, 5mM $NaClO_3$ were administrated to MCD (-) cells for induce their phenotype towards MCD (+) patient isolated cells. Due to MMP levels, fibronectin, one of the extracellular matrix proteins, is expressed at a low level in MCD (+) cells. In the injury model, similar results were observed for both FN1 and MMP levels for the 50mM concentration (Figure 27A – D). According to collagen expression level accumulation of collagen is increasing while MMP levels are decreasing (Figure 27E). CHST6 gene mutations cause MCD disease, and CHST6 expression levels are evaluated to better understand the effect of $NaClO_3$ on the injury model. Increasing $NaClO_3$ concentration has a similar expression levels with MCD (+) cells (Figure 27F). MCD (+) cells have lower levels of ALDH1A1 and ALDH3A1 gene expression than MCD (-) cells (Figure 27G and H). Following qPCR and ICC analyses, it was determined that a 7-day culture duration and a 50mM NaClO3 condition were acceptable as disease model.

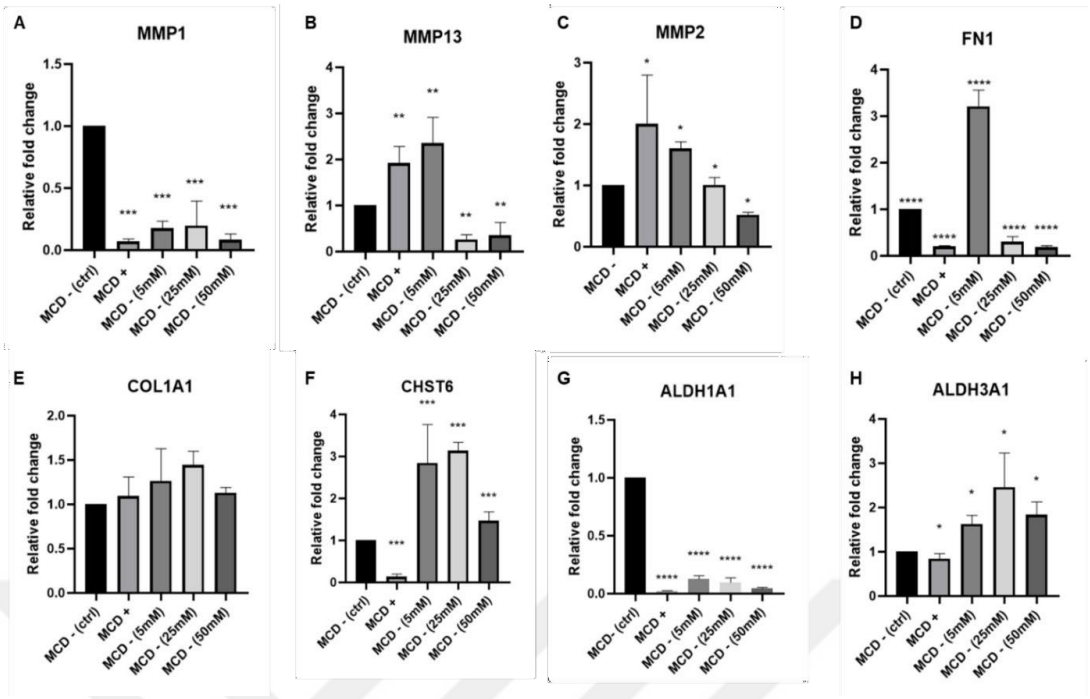

Figure 27 Expression of A-C) Matrix metalloproteinase 1, 13 and 2 D-E) Extracellular markers Fibronectin-1 and Collagen1A1, F) Macular Corneal Dystrophy gene CHST6, G-H) Corneal crystallins markers ALDH1A1 and ALDH3A1. The expression levels are compared to expression levels in the healthy primary cells. The values are normalized to GAPDH

4.5. Microfluidic Platform Design

Here we aim to develop a system that can mimic the aqueous humor pressure of anterior eye. The first experiments for the designed microfluidic platform were carried out with 3T3 cell line (Figure 28A). It was observed that 3T3 cells were not negatively affected by 7-day dynamic culture conditions (Figure 28B). The experiment was carried out using primary cells under the same culture conditions and no negative effects were seen on cell viability (Figure 28C).

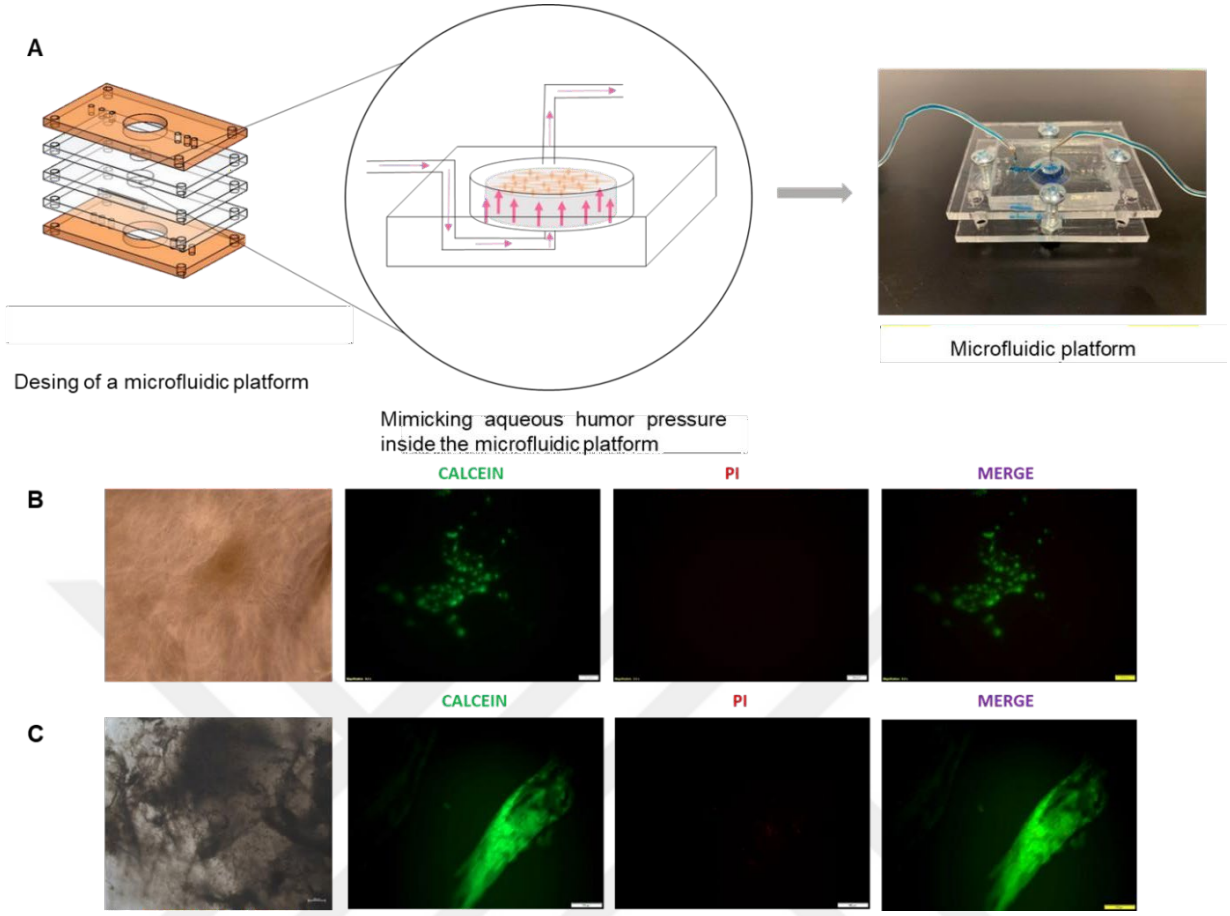

Figure 28 Microfluidic platform chip trails A) Microfluidic platform design B) 3T3 cell culturing inside the microfluidic platform for 7 days BF imaging and Calcein/PI stainings C) BF and Calcein/PI stainings after 7 days culturing of primary cells inside the microfluidic platform of primary cells inside the microfluidic platform.

4.6. Dynamic Disease Modelling

To create the disease model within the microfluidic platform, three groups were tested in dynamic culture conditions. In this study, three different groups were used. These are MCD (+) cells, MCD (-) cells, and the disease model created in previous studies with 50mM $NaClO_3$ concentration. After being cultured under flow for 7 days, histological analyses were performed.

Expression of different corneal stromal cell markers were detected with IHC (Figure 29 – Figure 33), indicating that MCD (+) cells and injury model maintained their characteristic during the dynamic culture conditions.

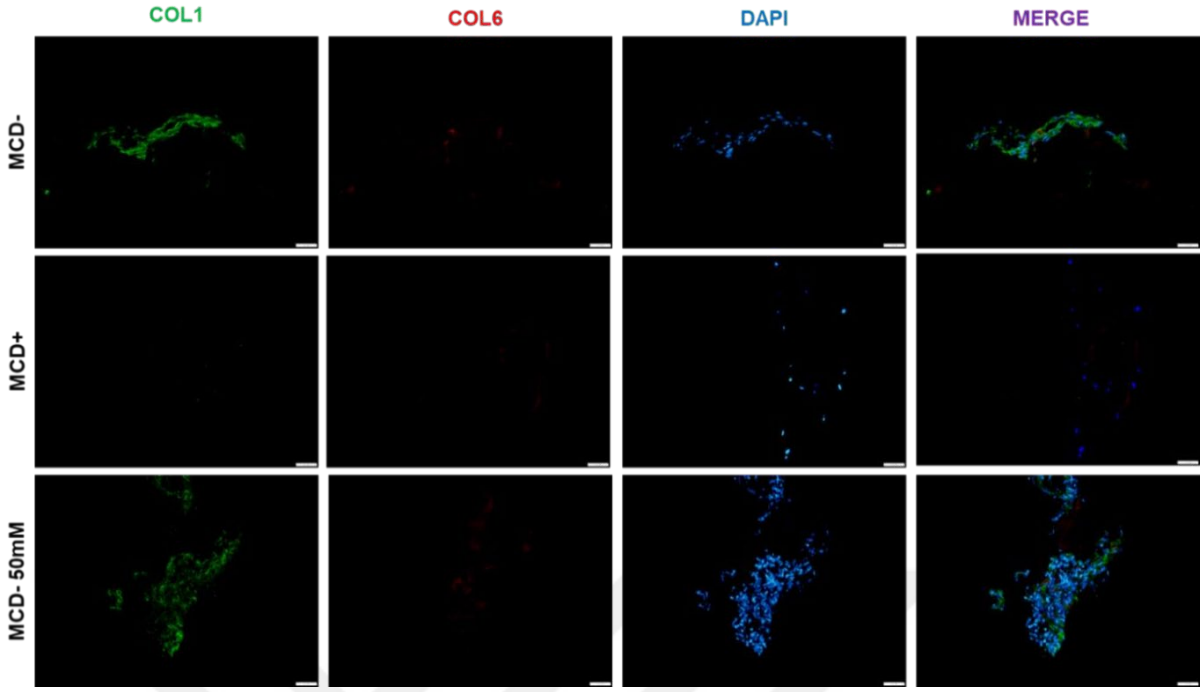

Figure 29 MCD (-), MCD (+) and NaClO3 treated groups stained against ECM markers Collagen I and Collagen VI. Nuclei are stained with DAPI.

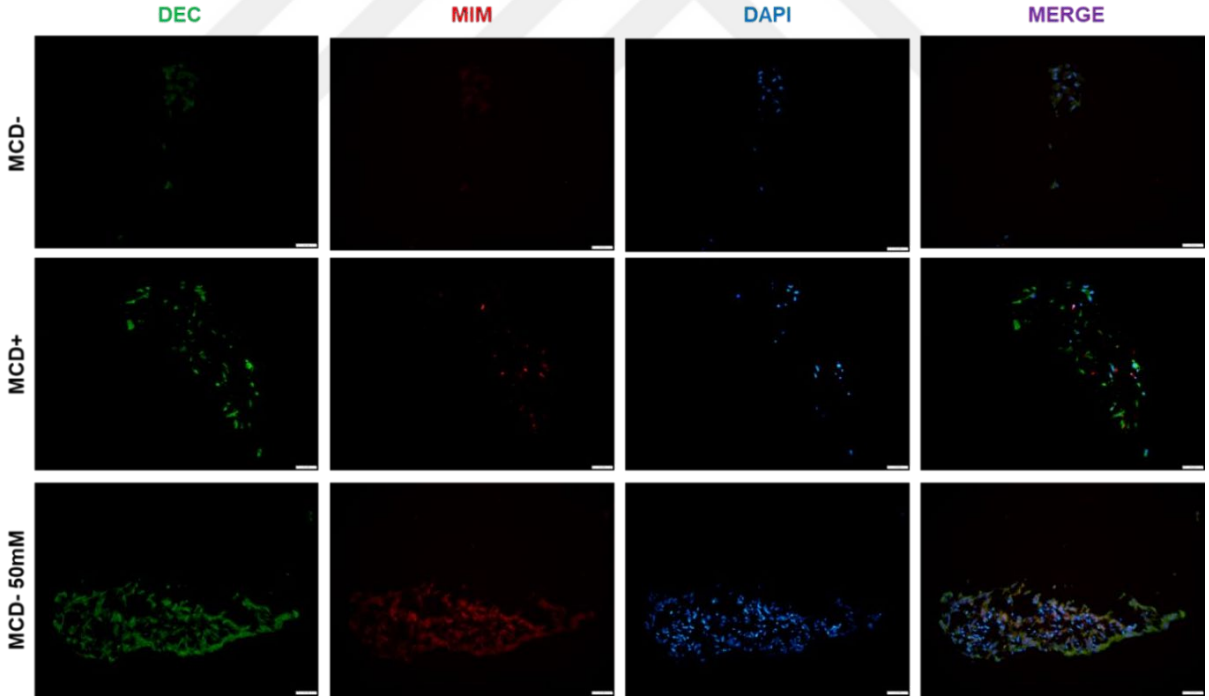

Figure 30 MCD (-), MCD (+) and $NaClO_3$ treated groups stained against corneal transparency markers Decorin (DEC) and Mimecan (MIM). Nuclei are stained with DAPI.

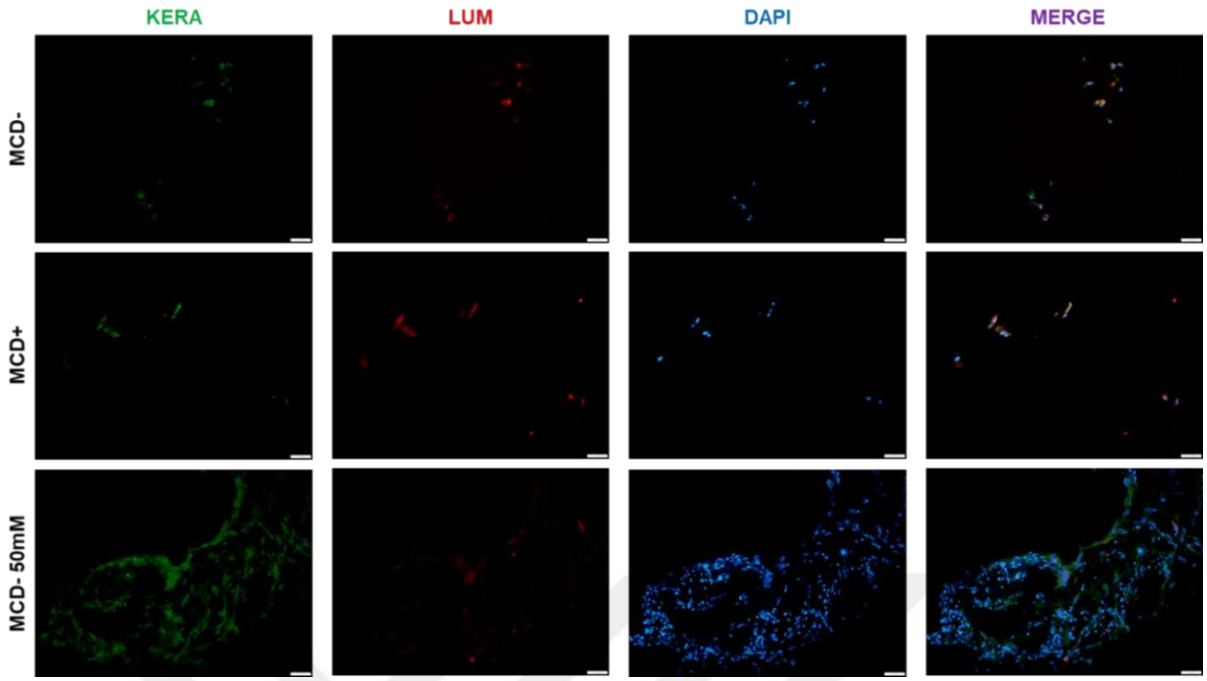

Figure 31 MCD (-), MCD (+) and NaClO3 treated groups stained against corneal transparency markers keratocan (KERA) and Lumican (LUM). Nuclei are stained with DAPI.

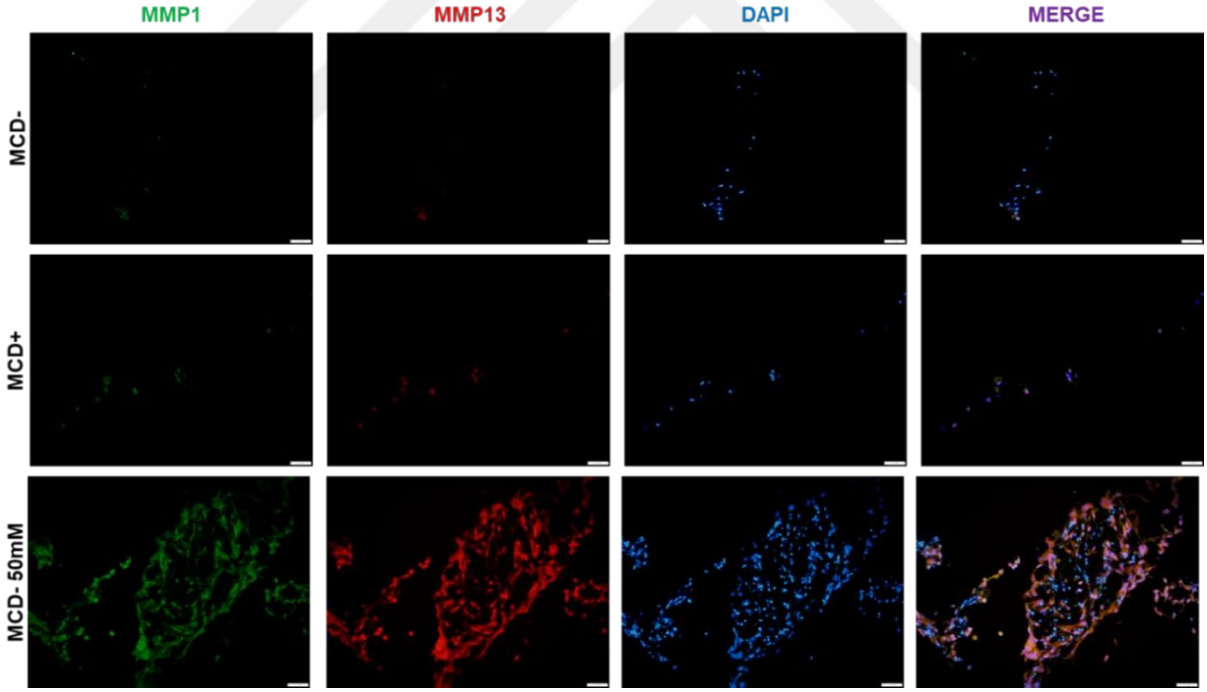

Figure 32 MCD (-), MCD (+) and NaClO3 treated groups stained against matrix metalloproteinase markers (MMP1 and MMP13). Nuclei are stained with DAPI.

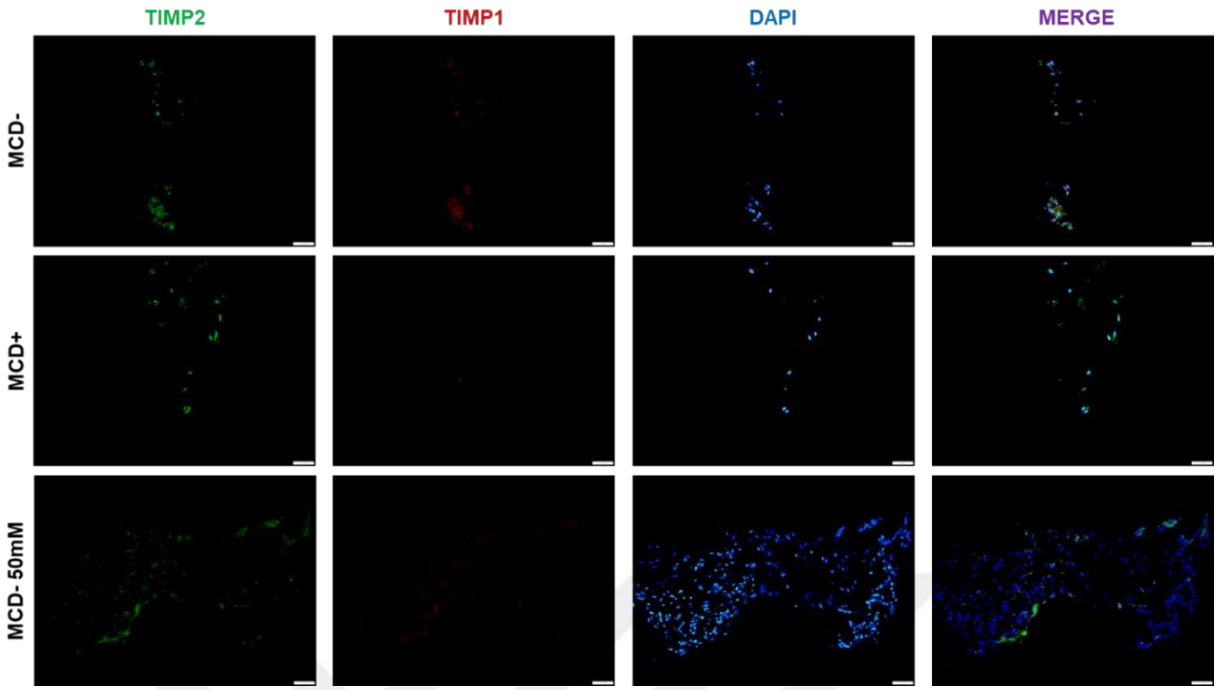

Figure 33 MCD (-), MCD (+) and NaClO3 treated groups stained against corneal remodeling markers (TIMP1 and TIMP2). Nuclei are stained with DAPI.

4.7. Alternative Treatment Methods

PrestoBlue was used to analyses the effects of recombinant MMP1 and MMP13 enzymes on cell viability in primary cells. The same experiment was later performed on MCD (+) cells as well. Results of cell viability assay of enzymes applied at different doses for 24 hours and 48 hours and there were no significant negative effects were observed on the cells (Figure 29).

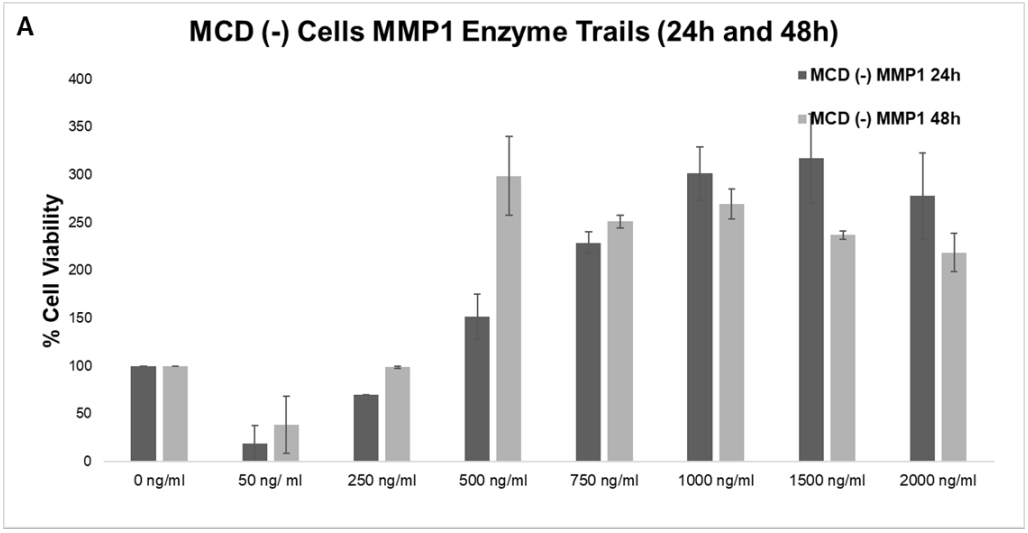
A
MCD (-) Cells MMP1 Enzyme Trails (24h and 48h)
MCD (-) MMP1 24h
MCD (-) MMP1 48h
% Cell Viability
400
350
300
250
200
150
100
50
0
0 ng/ml
50 ng/ ml
250 ng/ml
500 ng/ml
750 ng/ml
1000 ng/ml
1500 ng/ml
2000 ng/ml

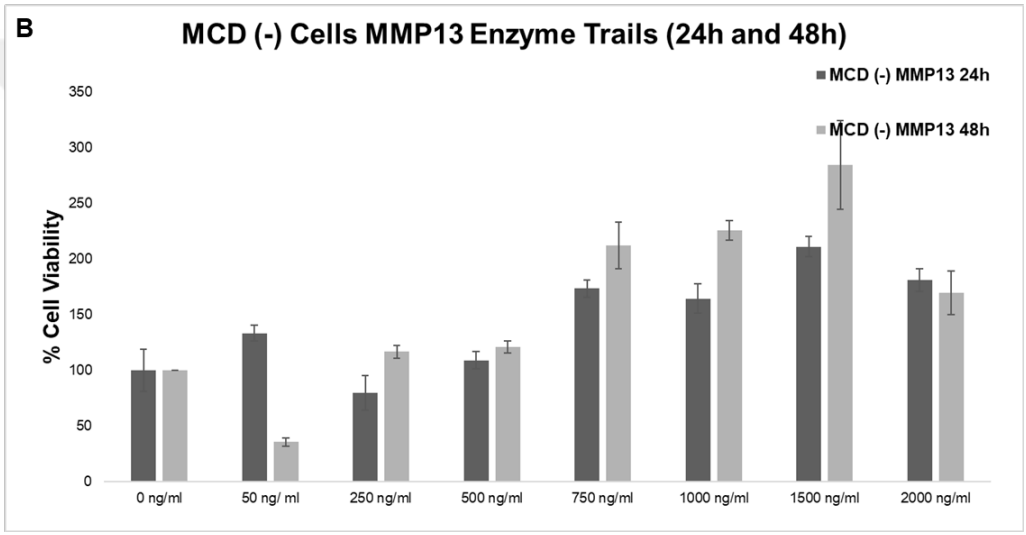
B
MCD (-) Cells MMP13 Enzyme Trails (24h and 48h)
MCD (-) MMP13 24h
MCD (-) MMP13 48h
% Cell Viability
350
300
250
200
150
100
50
0
0 ng/ml
50 ng/ ml
250 ng/ml
500 ng/ml
750 ng/ml
1000 ng/ml
1500 ng/ml
2000 ng/ml

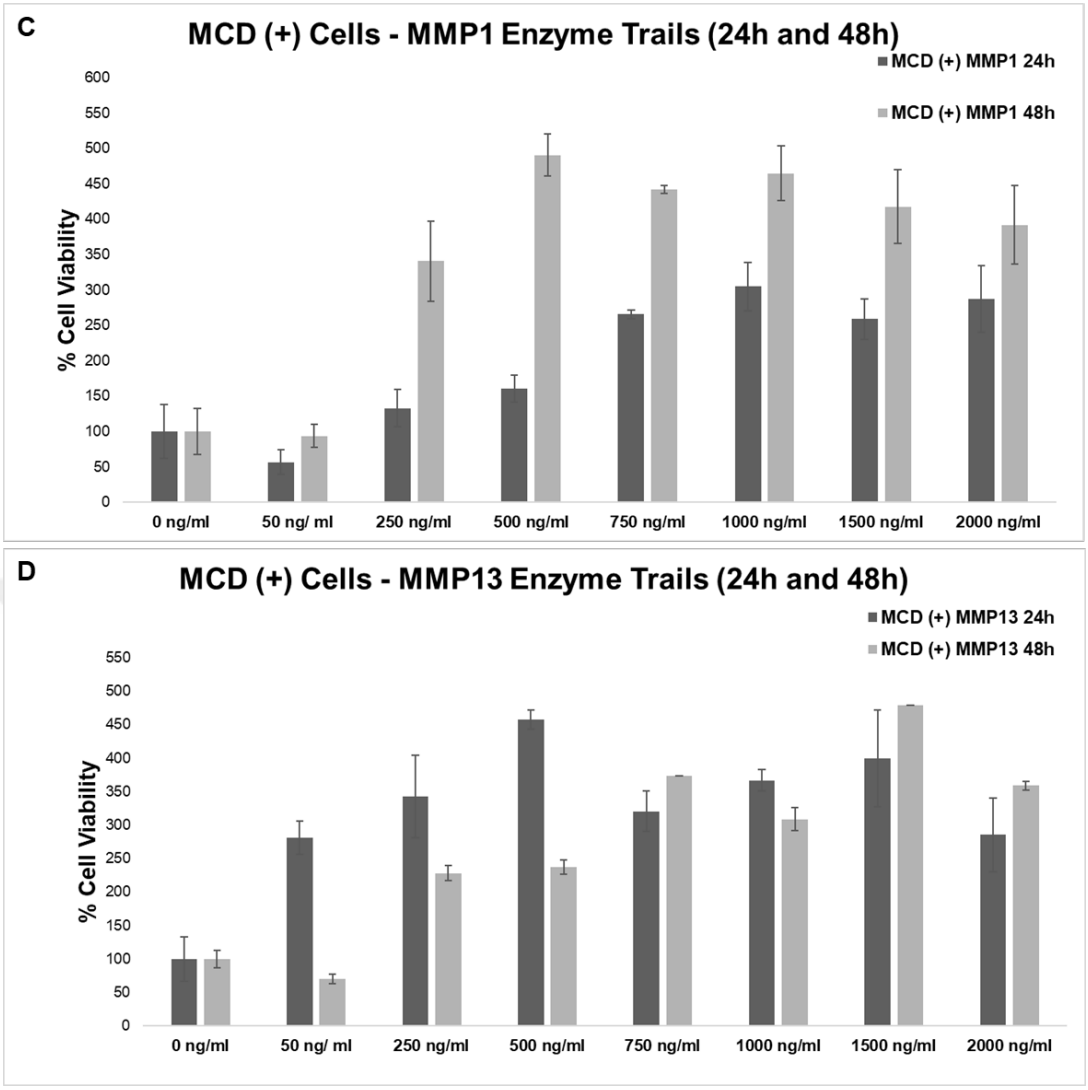

Figure 34 Cell Viability analyses of recombinant enzymes A and B) MCD (-) primary cells MMP1 and MMP13 enzyme trails for 24h and 48h C and D) MCD (+) primary cells MMP1 and MMP13 enzyme trails for 24h and 48h.

Three different enzyme concentrations were chosen based on the literature (Bozzelli et al., 2019) (Przybyla et al., 2013). Their therapeutic effects on MCD+ cells were tested and ALDH1A1, MMP1, MMP13, COL1A1, CHST6 and Fibronectin 1 genes mRNA expression levels were analyzed using qPCR analysis. When comparing the healthy group with MCD (+) cells, the expression levels change due the given treatment and they become closer to the control group (Figure 35 and Figure 36).

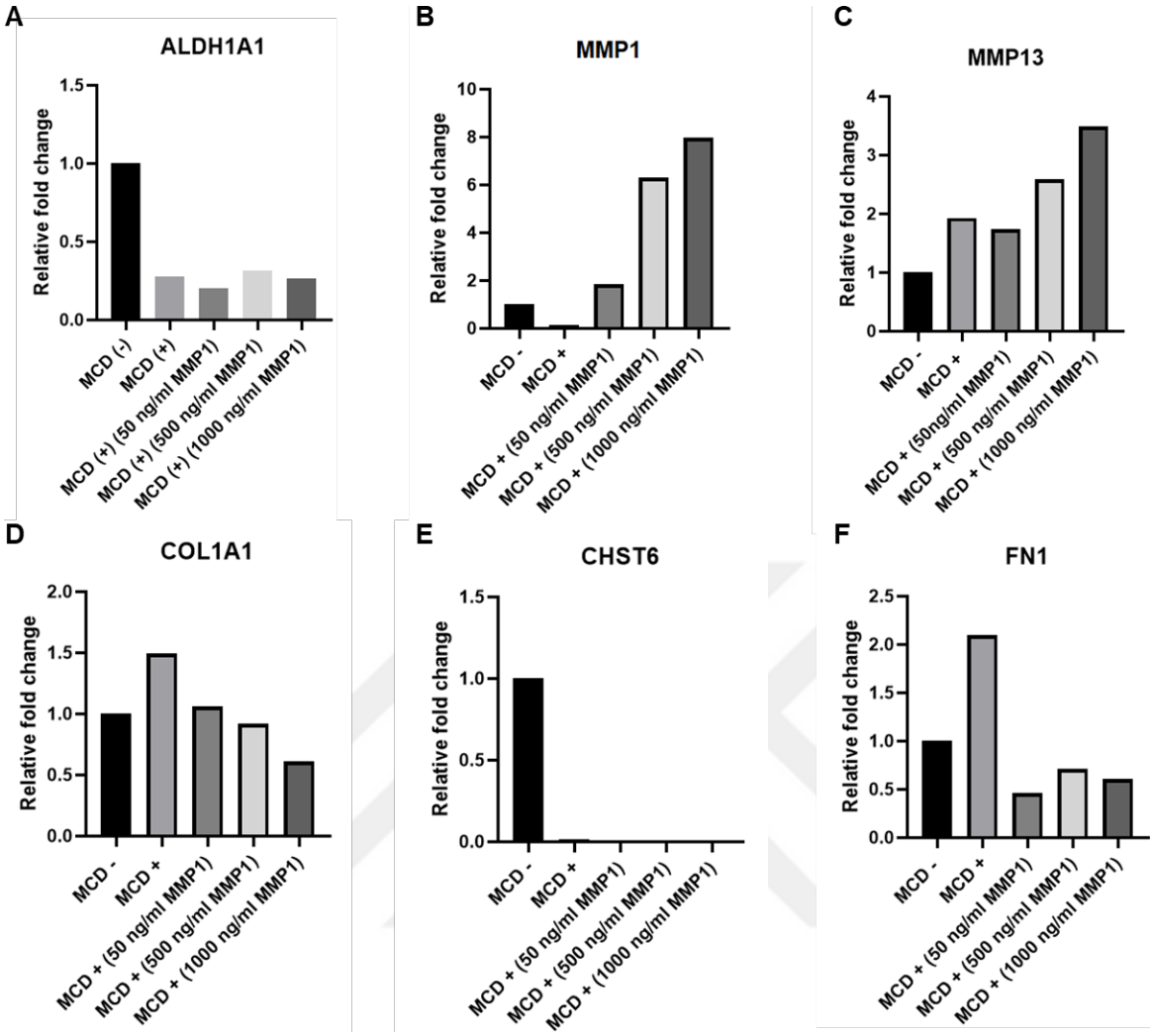

Figure 35 Expression of A) Corneal crystalline markers ALDH1A1 B-C) Matrix metalloproteinase 1, 13, D) Extracellular marker Collagen1A1 E) Macular Corneal Dystrophy gene CHST6 and F) Extracellular marker Fibronectin 1. The expression levels are compared to expression levels in the healthy primary cells. The values are normalized to GAPDH

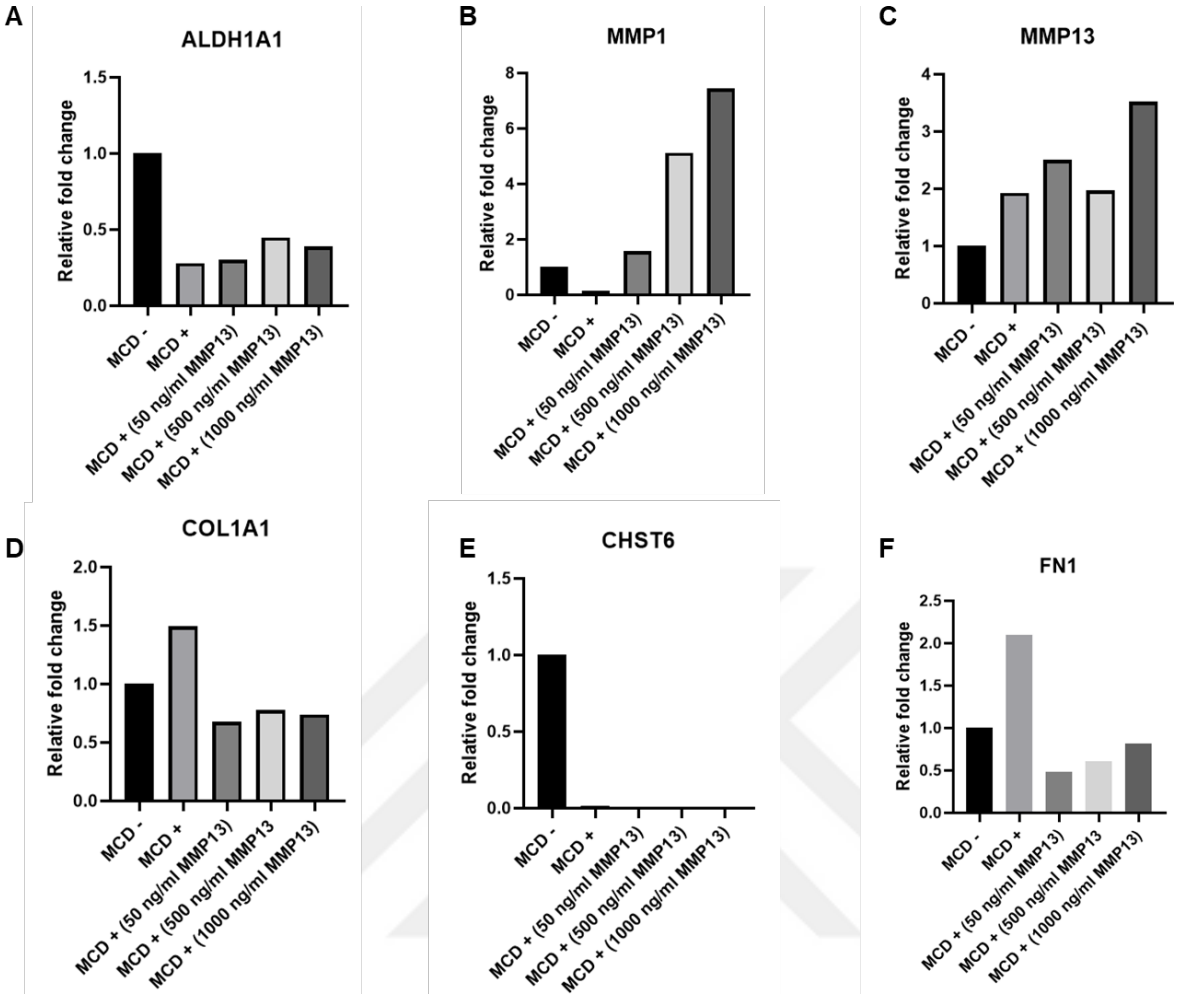

Figure 36 Expression of A) Corneal crystalline markers ALDH1A1 B-C) Matrix metalloproteinase 1, 13, D) Extracellular marker Collagen1A1 E) Macular Corneal Dystrophy gene CHST6 and F) Extracellular marker Fibronectin 1. The expression levels are compared to expression levels in the healthy primary cells. The values are normalized to GAPDH.

5. DISCUSSION

In this study, keratocytes from the human cornea were isolated and modeled for MCD disease via carrier hydrogel and microfluidic technology. To understand the progression of rare diseases and develop novel therapeutic strategies, *in vitro* disease models are needed. The significance of this study stems from the fact that MCD is a rare condition, and disease modeling studies using human keratocyte cells were not as common as other diseases in the cornea.

Our first aim was isolating the cells from human native cornea. For that purpose, literature review was conducted for primary keratocytes isolation from the human cornea. Four distinct protocols for keratocyte isolation were tested, namely DMEM F12 (SF), Comp. DMEM 5% FBS, DKSFM and Comp. DMEM 10% FBS. We observed that isolated human primary cells did not adhere in the serum-free medium, or low percentage of serum level (Figure 10 and Figure 11) (Murab et al., 2016) (Kureshi et al., 2014) (Gürdal et al., 2018). On the other hand, increasing the amount of serum increases cell adhesion and proliferation. It also appears that high serum percentage promotes also the adhesion and proliferation of MCD (+) cells (Figure 11). Phenotypic characterization of isolated keratocytes was accessed through cell specific immunoflurosecent stainings. Isolated and cultured keratocytes were positively stained for lumican, a glycoprotein found in stromal keratocytes of healthy corneas (C. Y. Liu & Kao, 2012). Also, Timp2 is a natural inhibitor of the matrix metalloproteinase family, and IF staining has shown its presence in cells isolated from healthy human cornea. We also detected keratocan in isolated cells, which is important for the organization and arrangement of the collagen matrix in the corneal stroma (Carlson et al., 2005). We showed that keratocytes cultured for 7 days secret cornea ECM positive for collagen I and collagen VI (Figure 12). Combining all, we validate cell isolation and culture protocols are suitable to source relevant cell types for the study.

To develop cell carrier hydrogel system based on gelatin, MPC and PEGDA. First, we aimed to assessed toxicity of the chemicals as well as observe the porosity of the material (Figure 14). Hydrogel synthesis has been the subject of numerous studies. Several different published protocols for hydrogel crosslinking were adapted and evaluated (Figure 15) (Islam et al., 2015) (Ahn et al., 2013) (Jangamreddy et al., 2018). Preliminary work done with gelatin to set and optimize the protocol for hydrogelsutilized in this study addressed the ratio of MPC and PEGDA to achieve a porous hydrogel architecture.

After getting experience from preliminary experiments, we started working with collagen. Our hydrogel generating technique based on the work of Islam et al, 2015 differs by utilizing collagen type I instead of collagen type III. Recombinant human collagen III integrated hydrogels demonstrate better mechanical and optical properties

when considered as an implantable graft. Since our main point is to develop an *in vitro* model rather than implantable graft use of collagen type I is advantageous in terms of abundancy, cost, and ease of use (W. Liu et al., 2008). Therefore, collagen type I was used as a carrier hydrogel instead of gelatin and its structure and rigidity was found to be suitable for further research (Figure 17). To assess toxicity of the collagen type I based hydrogel, we seeded 3T3 cells on the collagen hydrogel (Figure 18). Staining of Calcein/PI confirmed the cells viability after growing on collagen (Figure 19). Also isolated keratocytes were successfully cultured on collagen type I based hydrogel up to 8 days (Figure 20). Again, Calcein/PI staining confirmed this observation (Figure 21).

Following the cell viability examinations, we measured the water holding capacity of the collagen type I based hydrogels (Figure 22A). Water holding capacity of hydrogels shows porous structure and durability. The selected collagen based hydrogel water holding capacity is average at 30%, which is related to the small mesh size. This indicates that the produced hydrogel possesses a low water holding capacity and a more rigid structure. High rigidity helps us to handle the hydrogel more easily compared to the high water holding capacity hydrogels. To assess the stiffness of the developed collagen type I hydrogel, we performed a tensile-compression analysis. (Figure 22B). As expected, higher collagen ratio resulted in higher stiffness of the hydrogels. We observed that collagen hydrogel was rigid enough for handling and physical manipulation. This result facilitates future experiments since it allows us to handle and place cell seeded hydrogels inside microfluidic platform for dynamic settings. According to SEM results, as the collagen concentration is increased, the amount of collagen fibrils increases. The viability analyses of the cells that were cultivated in the hydrogel revealed that increasing collagen ratio is associated with higher cell adhesion. As a conclusion, among the different collagen ratios and crosslinking conditions, the most suitable hydrogel for cellular behavior and mechanical properties was Collagen Type I : MPC : PEG (7.5 : 1: 1.5) mixture (Figure 23).

$NaClO_3$ was utilized to stimulate healthy keratocytes *in vitro* in order to mimic MCD disease (Murab et al., 2016). Murab et al., conducted the research to develop *in*

vitro disease model using goat cornea cells. In this study we evaluate reported MCD model using human cornea cells. First, we check the viability level of primary cells for four different concentrations of $NaClO_3$ for 14 days. Even high concentration of $NaClO_3$ (50mM) and cultivation for 14 days' period did not result in decreased cell viability (Figure 24). After that, we used different concentrations of $NaClO_3$ on the cells we isolated from the human cornea and compared the results to the MCD (+) patient's cells. Evaluation of protein-levels through IF staining showed that different culture periods and different $NaClO_3$ concentration affected MMP1, MMP13 and collagen I intensities. Higher concentration of $NaClO_3$ led to decreased levels of MMP1 and MMP13. This effect was highest on day 7. Collagen I levels also decreased after exposure to increasing levels of $NaClO_3$ (Figure 25). We repeated the IF staining with MCD (+) cells (Figure 26). Unlike Murab et al., where they performed their experiments over a culture period of 14 days, we found that MCD (+) cells responded with similar decreased expression levels of MMP1, MMP13 and Collagen I after 7 days of cultivation. Evaluation of gene expression levels through qPCR confirmed the previous IF results. MMP markers and FN1 have similar expression pattern with MCD (+) cells and disease model as well (Figure 27).

MCD disease is a genetic disease caused by a mutation in the CHST6 gene. This mutation results in decreased levels of MMP's as well as corneal crystallins (ALDH1A1 and ALDH3A1). Evaluation of CHST6 gene expression levels showed lower CHST6 expression in MCD (+) isolated keratocytes compered to MCD (-) cells. The levels of ALDH1A1 and ALDH3A1 genes, which cause crystal appearance in the cornea, also decreased in MCD (+) as well as in MCD (-) treated with 50mM $NaClO_3$ (Figure 27).

Microfluidic platforms are excellent tools that can be used to recapitulate tissues and organs. These platforms enable the modelling and further examination of diseases. Here we developed a system that can mimic the aqueous humor pressure of anterior eye, thereby cells used in MCD model will be exposed to dynamic conditionand mechanical stimulation (Figure 28A). Both the 3T3 cell line and primary keratocytes were seeded on hydrogel within the microfluidic platform. To assess the viability of cells inside the microfluidic platform we performed Calcein/PI stainings. Weobserved that the dynamic condition had no negative effect on both 3T3 and

keratocytes cell viability (Figure 28B and 28C). After seeding as droplets on the developed hydrogel, isolated MCD (+) and MCD (-) primary cells were cultured under dynamic conditions for 7 days. In a dynamic model, $NaClO_3$ was administrated to MCD (-) cells. We prepared histological sections of the cells seeded on the hydrogels. Unfortunately, the cell density was not as high as expected. This could be due to the primary cells having been negatively affected by the 7-day dynamic culture period. For this reason, no definite conclusion about expression levels of Col I, Col VI, Decorin, Mimecan, keratocan, Lumican, MMP1, MMP13, TIMP1 and TIMP2 could be drawn (Figure 29 – Figure 33).

MMP1 and MMP13 plays a function in corneal matrix remodeling and the expression levels of enzymes have been reported to decrease in macular degenerations (Daniels et al., 2003) (Ye et al., 2000). In our model, we wanted to evaluate an alternative approach for the treatment of MCD disease with MMP1 and MMP13 enzymes replacement therapy. Seven different concentrations (50 ng/ml, 250 ng/ml, 500 ng/ml, 750 ng/ml, 1000 ng/ml, 1500 ng/ml and 2000 ng/ml) of MMP1 and MMP13 were examined before choosing the proper doses for the enzyme study. MMP 1 and MMP 13 enzymes were studied by Bozzelli et al., 2019 and Przybyla et al., 2013 and we refer to their studies in terms of the determine the enzyme concentrations. (Figure 34). We determine the IC_{50} value of the highest concentration (2000 ng/ml) of MMP1 and MMP13. We confirmed that even high doses of enzymes do not significantly affect cell viability (Figure 34). Prior of microfluidic platform experiments, effect of enzymes on MCD (+) cells was assessed in conventional culture system. For that, MCD (+) cells were seeded on 6 - well plate and administrated 50, 500, 1000 ng/ml ofMMP1 and MMP13 separately. Expression levels of ALDH1A1, MMP1, MMP13,COL1A1, CHST6 and FN1 were analyzed. The results were compared to healthy groups to see whether the enzyme groups' expression levels match those of the MCD(-) groups. We expected to see a decrease in collagen (COL1A1) since MMP1 and MMP13 possess a digestive function for collagen. As a consequence of this, we expected increasing expression levels of crystalline (ALDH1A1). Indeed, we saw a decrease of collagen expression in MCD (+) cells treated with both MMP1 and MMP13.However, ALDH1A1 expression in MCD (+) was not affected by MMP1 and MMP13 treatment. Finally, we observed increasing MMP1 and MMP13 expression levels in

MCD (+) cells when treated with either MMP1 or MMP13. This suggests a possible correlation between MMP1 and MMP13 enzyme activity.

6. CONCLUSION AND FUTURE PERSPECTIVES

In this study, we successfully developed a bioengineered MCD *in vitro* disease model using MCD (+) positive patients' cells and carrier collagen based hydrogels. We observed similar results when comparing the characteristics of patients isolated MCD (+) cells with MCD (-) cells treated with $NaClO_3$ as an injury model. This indicates that the disease can be mimicked using this injury model.

As an alternative treatment approach, enzyme replacement therapy was performed. According to gene expression analysis, the replacement therapy had positive effect on MCD (+) cells.

It is clear that if the results of the dynamic system are repeated, the model will be significantly improved. The effect of treatment can be better understood with a complete IF analysis at this point. Despite the fact that the system is dynamic, there are multiple parameters in the eye that mimic the disease. To better understand the effect of the MCD, a MCD (+) organoid model on carrier hydrogel inside microfluidic platforms could be created in the future.

7. REFERENCES

Ahn, J. I., Kuffova, L., Merrett, K., Mitra, D., Forrester, J. V., Li, F., & Griffith, M. (2013). Crosslinked collagen hydrogels as corneal implants: effects of sterically bulky vs. non-bulky carbodiimides as crosslinkers. *Acta biomaterialia*, *9*(8), 7796-7805.

Baratta, R. O., Schlumpf, E., Del Buono, B. J., DeLorey, S., & Calkins, D. J. (2022). Corneal collagen as a potential therapeutic target in dry eye disease. *Survey of Ophthalmology*, *67*(1), 60-67.

Blackburn, B. J., Jenkins, M. W., Rollins, A. M., & Dupps, W. J. (2019). A review of structural and biomechanical changes in the cornea in aging, disease, and photochemical crosslinking. *Frontiers in bioengineering and biotechnology*, *7*, 66.

Bozzelli, P. L., Yin, T., Avdoshina, V., Mocchetti, I., Conant, K. E., & Maguire-Zeiss, K. A. (2019). HIV-1 Tat promotes astrocytic release of CCL2 through MMP/PAR-1 signaling. *Glia*, *67*(9), 1719-1729.

Carlson, E. C., Liu, C. Y., Chikama, T. I., Hayashi, Y., Kao, C. W. C., Birk, D. E., ... & Kao, W. W. Y. (2005). Keratocan, a Cornea-specific Keratan Sulfate Proteoglycan, Is Regulatedby Lumican. *Journal of Biological Chemistry*, *280*(27), 25541-25547.

Chakravarti, S., Petroll, W. M., Hassell, J. R., Jester, J. V., Lass, J. H., Paul, J., & Birk, D. E. (2000). Corneal opacity in lumican-null mice: defects in collagen fibril structure and packing in the posterior stroma. *Investigative ophthalmology & visual science*, *41*(11), 3365-3373.

Chen, Z., You, J., Liu, X., Cooper, S., Hodge, C., Sutton, G., ... & Wallace, G. G. (2018). Biomaterials for corneal bioengineering. *Biomedical Materials*, *13*(3), 032002.

Daniels, J. T., Limb, G. A., Saarialho-Kere, U., Murphy, G., & Khaw, P. T. (2003). Human corneal epithelial cells require MMP-1 for HGF-mediated migration on collagen I. Investigative ophthalmology & visual science, 44(3), 1048-1055.

Di Iorio, E., Barbaro, V., Volpi, N., Bertolin, M., Ferrari, B., Fasolo, A., ... & Ferrari, S. (2010). Localization and expression of CHST6 and keratan sulfate proteoglycans in the human cornea. *Experimental eye research*, *91*(2), 293-299.

Espana, E. M., & Birk, D. E. (2020). Composition, structure and function of the corneal stroma. *Experimental Eye Research*, *198*, 108137.

Gürdal, M., Barut Selver, Ö., Baysal, K., & Durak, İ. (2018). Comparison of culture media indicates a role for autologous serum in enhancing phenotypic preservation of rabbit limbal stem cells in explant culture. *Cytotechnology*, *70*(2), 687-700.

Hongqing, Q. Y., Maeda, M., Fu-Shin, X. Y., & Azar, D. T. (2000). Differential expression of MT1-MMP (MMP-14) and collagenase III (MMP-13) genes in normal and wounded rat corneas. Investigative ophthalmology & visual science, 41(10), 2894-2899.

Huh, D., Leslie, D. C., Matthews, B. D., Fraser, J. P., Jurek, S., Hamilton, G. A., ... & Ingber, D. E. (2012). A human disease model of drug toxicity-induced pulmonary edema in a lung-on-a-chip microdevice. *Science translational medicine*, *4*(159), 159ra147-159ra147.

Islam, M. M., Cėpla, V., He, C., Edin, J., Rakickas, T., Kobuch, K., ... & Griffith, M. (2015). Functional fabrication of recombinant human collagen-phosphorylcholine hydrogels for regenerative medicine applications. *Acta biomaterialia*, *12*, 70-80.

Islam, M. M., Ravichandran, R., Olsen, D., Ljunggren, M. K., Fagerholm, P., Lee, C. J., ... & Phopase, J. (2016). Self-assembled collagen-like-peptide implants as alternatives to human donor corneal transplantation. *RSC advances*, *6*(61), 55745- 55749.

Jabłońska-Trypuć, A., Matejczyk, M., & Rosochacki, S. (2016). Matrix metalloproteinases (MMPs), the main extracellular matrix (ECM) enzymes in collagen degradation, as a target for anticancer drugs. *Journal of enzyme inhibition and medicinal chemistry*, *31*(sup1), 177-183.

Jalili-Firoozinezhad, S., Miranda, C. C., & Cabral, J. M. (2021). Modeling the human body on microfluidic chips. *Trends in Biotechnology*, *39*(8), 838-852.

Jangamreddy, J. R., Haagdorens, M. K., Islam, M. M., Lewis, P., Samanta, A., Fagerholm, P., ... & Griffith, M. (2018). Short peptide analogs as alternatives to collagen in pro-regenerative corneal implants. *Acta biomaterialia*, *69*, 120-130.

Kadakia, A., Keskar, V., Titushkin, I. A., Djalilian, A., Gemeinhart, R. A., & Cho, M. (2008). Hybrid superporous scaffolds: an application for cornea tissue engineering. *Critical Reviews™ in Biomedical Engineering*, *36*(5-6).

Keane, M., Coster, D., Ziaei, M., & Williams, K. (2014). Deep anterior lamellar keratoplasty versus penetrating keratoplasty for treating keratoconus. *Cochrane Database of Systematic Reviews*, (7).

Klintworth, G. K. (2009). Corneal dystrophies. *Orphanet journal of rare diseases*, *4*(1), 1-38.

Kowalski, G., Kijowska, K., Witczak, M., Kuterasiński, Ł., & Łukasiewicz, M. (2019). Synthesis and effect of structure on swelling properties of hydrogels based on high methylated pectin and acrylic polymers. Polymers, 11(1), 114.

Kureshi, A. K., Funderburgh, J. L., & Daniels, J. T. (2014). Human Corneal Stromal Stem Cells Exhibit Survival Capacity Following Isolation From Stored Organ-Culture Corneas. *Investigative ophthalmology & visual science*, *55*(11), 7583-7588.

Lee, J. T. Y., & Chow, K. L. (2012). SEM sample preparation for cells on 3D scaffolds by freeze-drying and HMDS. *Scanning*, *34*(1), 12-25.

Lee, Y. K., Chang, D. J., & Chung, S. K. (2013). A case of Korean patient with macular corneal dystrophy associated with novel mutation in the CHST6 gene. Korean Journal of Ophthalmology, 27(6), 454-458.

Liu, C. Y., & Kao, W. W. Y. (2012). Lumican promotes corneal epithelial wound healing. In *Proteoglycans* (pp. 285-290). Humana Press.

Liu, C. Y., Birk, D. E., Hassell, J. R., Kane, B., & Kao, W. W. Y. (2003). Keratocan-deficient mice display alterations in corneal structure. *Journal of Biological Chemistry*, *278*(24), 21672-21677.

Liu, W., Merrett, K., Griffith, M., Fagerholm, P., Dravida, S., Heyne, B., ... & Li, F. (2008). Recombinant human collagen for tissue engineered corneal substitutes. *Biomaterials*, *29*(9), 1147-1158.

Liu, Y., Gan, L., Carlsson, D. J., Fagerholm, P., Lagali, N., Watsky, M. A., ... & Griffith, M. (2006). A simple, cross-linked collagen tissue substitute for corneal implantation. *Investigative ophthalmology & visual science*, *47*(5), 1869-1875.

Mahdavi, S. S., Abdekhodaie, M. J., Mashayekhan, S., Baradaran-Rafii, A., & Djalilian, A. R. (2020). Bioengineering approaches for corneal regenerative medicine. *Tissue engineering and regenerative medicine*, *17*(5), 567-593.

Masterton, S., & Ahearne, M. (2018). Mechanobiology of the corneal epithelium. *Experimental eye research*, *177*, 122-129.

Meek, K. M., & Boote, C. (2004). The organization of collagen in the corneal stroma. *Experimental eye research*, *78*(3), 503-512.

Meeney, A., & Mudhar, H. S. (2013). Histopathological reporting of corneal pathology by a biomedical scientist: the Sheffield Experience. *Eye*, *27*(2), 272-276.

Merrett, K., Fagerholm, P., McLaughlin, C. R., Dravida, S., Lagali, N., Shinozaki, N., ... & Griffith, M. (2008). Tissue-engineered recombinant human collagen-based corneal substitutes for implantation: performance of type I versus type III collagen. *Investigative ophthalmology & visual science*, *49*(9), 3887-3894.

Michelacci, Y. M. (2003). Collagens and proteoglycans of the corneal extracellular matrix. *Brazilian Journal of Medical and Biological Research*, *36*(8), 1037-1046.

Miyashita, H., Shimmura, S., Kobayashi, H., Taguchi, T., Asano-Kato, N., Uchino, Y., ... & Tsubota, K. (2006). Collagen-immobilized poly (vinyl alcohol) as an artificial cornea scaffold that supports a stratified corneal epithelium. *Journal of Biomedical Materials Research Part B: Applied Biomaterials: An Official Journal of The Society for*

Biomaterials, The Japanese Society for Biomaterials, and The Australian Society for Biomaterials and the Korean Society for Biomaterials, *76*(1), 56-63.

Murab, S., Chameettachal, S., & Ghosh, S. (2016). Establishment of an in vitro monolayer model of macular corneal dystrophy. *Laboratory Investigation*, *96*(12), 1311-1326.

Nosrati, H., Alizadeh, Z., Nosrati, A., Ashrafi-Dehkordi, K., Banitalebi-Dehkordi, M., Sanami, S., & Khodaei, M. (2021). Stem cell-based therapeutic strategies for corneal epithelium regeneration. *Tissue and Cell*, *68*, 101470.

Ozcelik, B., Brown, K. D., Blencowe, A., Daniell, M., Stevens, G. W., & Qiao, G. G. (2013). Ultrathin chitosan–poly (ethylene glycol) hydrogel films for corneal tissue engineering. *Acta biomaterialia*, *9*(5), 6594-6605.

Palchesko, R. N., Carrasquilla, S. D., & Feinberg, A. W. (2018). Natural biomaterials for corneal tissue engineering, repair, and regeneration. *Advanced healthcare materials*, *7*(16), 1701434.

Przybyla, L. M., Theunissen, T. W., Jaenisch, R., & Voldman, J. (2013). Matrix remodeling maintains embryonic stem cell self-renewal by activating stat3. *Stem cells*, *31*(6), 1097-1106.

Quantock, A. J., Young, R. D., & Akama, T. O. (2010). Structural and biochemical aspects of keratan sulphate in the cornea. *Cellular and molecular life sciences*, *67*(6), 891-906.

Ren, K., Zhou, J., & Wu, H. (2013). Materials for microfluidic chip fabrication. *Accounts of chemical research*, *46*(11), 2396-2406.

Seo, J., Byun, W. Y., Alisafaei, F., Georgescu, A., Yi, Y. S., Massaro-Giordano, M., ... & Huh, D. (2019). Multiscale reverse engineering of the human ocular surface. *Nature medicine*, *25*(8), 1310-1318.

Seyed, M. A., & Vijayaraghavan, K. (2018). Physicochemical characterization and bioactivity of an improved chitosan scaffold cross-linked with polyvinyl alcohol for corneal tissue engineering applications. *Annual Research & Review in Biology*, 1-16.

Singh, S., Das, S., Kannabiran, C., Jakati, S., & Chaurasia, S. (2021). Macular corneal dystrophy: an updated review. *Current Eye Research*, *46*(6), 765-770.

Singhal, D., Sahay, P., Goel, S., Asif, M. I., Maharana, P. K., & Sharma, N. (2020). Descemet membrane detachment. *Survey of ophthalmology*, *65*(3), 279-293.

Sridhar, M. S. (2018). Anatomy of cornea and ocular surface. *Indian journal of ophthalmology*, *66*(2), 190.

Tuft, S. J., and D. J. Coster. "The corneal endothelium." Eye 4.3 (1990): 389-424.

Uchino, Y., Shimmura, S., Miyashita, H., Taguchi, T., Kobayashi, H., Shimazaki, J., ... & Tsubota, K. (2007). Amniotic membrane immobilized poly (vinyl alcohol) hybrid polymer as an artificial cornea scaffold that supports a stratified and differentiated corneal epithelium. *Journal of Biomedical Materials Research Part B: Applied Biomaterials: An Official Journal of The Society for Biomaterials, The Japanese Society for Biomaterials, and The Australian Society for Biomaterials and the Korean Society for Biomaterials*, *81*(1), 201-206.

Weiss, J. S., Møller, H. U., Aldave, A. J., Seitz, B., Bredrup, C., Kivelä, T., ... & Lisch, W. (2015). IC3D classification of corneal dystrophies–edition 2. *Cornea*, *34*(2), 117-159.

Willoughby, C. E., Ponzin, D., Ferrari, S., Lobo, A., Landau, K., & Omidi, Y. (2010). Anatomy and physiology of the human eye: effects of mucopolysaccharidoses disease on structure and function-a review. *Clinical & Experimental Ophthalmology*, *38*, 2-11.

Wilson, S. E. (2020). Bowman's layer in the cornea-structure and function and regeneration. *Experimental eye research*, *195*, 108033.

Zhang, L., Anderson, M. C., & Liu, C. Y. (2017). The role of corneal stroma: A potential nutritional source for the cornea. *Journal of nature and science*, *3*(8).

8. APPENDIX

8.1. Patient Consent Form

BİLGİLENDİRİLMİŞ GÖNÜLLÜ OLUR FORMU

Araştırmanın Adı: Maküler Kornea Distrofisi için yeni bir topikal tedavi yönteminin geliştirilmesi

Araştırmayı yapan kişi/kurum: Araştırma Dokuz Eylül Üniversitesi Tıp Fakültesi Göz Hastalıkları Anabilim Dalı'na "Kornea Nakli" için başvuran hastalardan oluşacaktır. Çalışma Göz Hastalıkları Anabilim Dalı'dan Doç.Dr Aslı YILDIRIM tarafından İzmir Biyotıp ve Genom Merkezi'nde yürütülecektir.

Araştırmanın Amacı Nedir ?

Bu projenin amacı nadir bir genetik hastalık olan maküler kornea distrofisi'nin (MKD) moleküler mekanizmasına dayanan yeni bir tedavi yönteminin geliştirilmesidir. Bu proje ile MKD için kornea nakli ihtiyacını ortadan kaldıran bir göz damlası tedavisi geliştirilmesi hedeflenmektedir

Bu amaçla, sizlerden halihazırda alınacak olan ve bir daha kullanılmayacak olan korneaları çalışmamızda kullanmak üzere talep etmekteyiz.

Katılma Koşulları Nedir?

Bu çalışmaya Dokuz Eylül Üniversitesi Tıp Fakültesi Göz Hastalıkları Anabilim Dalı'na başvuran ve kornea nakli yapılacak olan hastalar dahil edilecektir.

Nasıl Bir Uygulama Yapılacaktır?

MKD veya korneada nedbe dokusu (skar) / şekil bozukluğu nedeniyle görme tashihi amacıyla gerçekleştirilen kornea nakilleri sonrası açığa çıkan morfolojik yapısı bozulmamış kornea dokuları kullanılacaktır. Hali hazırda nakil işlemi için operasyona alınan hastalardan cerrahi işlem esnasında zaten çıkarılacak ve bir daha kullanılmayacak kornealar bu çalışma için ayrılacaktır.

Sorumluluklarım Nelerdir?

Araştırma ile ilgili olarak sizin sorumluluklarınız yoktur.

Katılımcı Sayısı Nedir?

Dokuz Eylül Üniversitesi Göz Hastalıkları Anabilim Dalı'na kornea nakli için başvuran hasta sayısı kadar katılımcıdan oluşacaktır.

Katılımım Ne Kadar Sürecek?

Bu çalışmada yer almanız için ön görülen süre yoktur.

Çalışmaya Katılma ile Beklenen Olası Yararlar Nelerdir?

Bu araştırmada sizin için beklenen yararlar ya da zararlar yoktur. Bilime katkı sağlayabilecektir.

Çalışmaya Katılma ile Beklenen Olası Riskler Nelerdir?

Ameliyat esnasından yapılacak girişim dışında ilave bir müdahelede bulunulmayacaktır. Bu yüzden olası bir risk yoktur.

Hangi Koşullarda Araştırma Dışı Bırakılabilirim ?

Çalışma materyali yetersiz olduğunda, çalışmacı sizin izniniz olmadan sizi çalışmadan çıkarabilir.

Çalışma Kapsamında Giderler Karşılanacak Mı ?

Çalışma sırasında gerekli olan işlemlerin masrafı size veya güvencesi altında bulunduğunuz resmi ya da özel hiçbir kurum veya kuruluşa ödetilmeyecektir.

Çalışmayı Destekleyen Kurum Var Mıdır?

Çalışmamız TÜBİTAK 1003 projesi kapsamında TÜBİTAK tarafından desteklenmektedir.

Çalışmaya Katılmam Nedeniyle Tarafıma Herhangi Bir Ödeme Yapılacak Mıdır?

Bu araştırmada yer almanız nedeniyle size hiçbir ödeme yapılmayacaktır.

Katılmama İlişkin Bilgiler Konusunda Gizlilik Sağlanabilecek Mi?

Bu çalışmayla bağlantılı olarak elde edilen ve sizinle özdeşleşmiş her bilgi gizli kalacak, 3. kişilerle paylaşılmayacak ve yalnızca sizin izniniz veya kanunun gerektirdiği ölçüde ifşa edilecektir. Gizlilik tanımlanmış bir kodlama prosedürüyle sağlanacak ve kod çözümüne erişim yalnızca çalışmanın sorumlusu olan araştırmacıyla sınırlı kalacaktır. Tüm veriler, sınırlı erişime sahip güvenli ve şifreli bir bilgisayarda tutulacaktır.

Araştırmaya Katılmayı Kabul Etmemem Veya Araştırmadan Ayrılmam Durumunda Ne Yapmam Gerekir?

Bu çalışmanın içinde olmak isteyip istemediğinize etki altında kalmadan, bağımsızca karar verebilirsiniz. Bu çalışmaya gönüllü olarak katılmaya karar vermeniz halinde dahi, sahip olduğunuz herhangi bir hakkı kaybetmeden veya herhangi bir cezaya maruz kalmadan istediğiniz zaman çekilebilirsiniz. Çalışmadan çekilmek istemenizin ceza karşılığı yoktur ve sahip olduğunuz faydaları kaybetmiş olmazsınız. Bu çalışmaya katılmayla ilgili kararınız, tedavinizi veya doktorunuzla olan ilişkinizi hiç bir şekilde etkilemeyecektir.

Hastanın Beyanı

Yukarıda yer alan ve araştırmaya başlanmadan önce gönüllüye verilmesi gereken bilgileri gösteren 2 sayfalık metni okudum ve sözlü olarak dinledim. Aklıma gelen tüm soruları araştırıcıya sordum, yazılı ve sözlü olarak bana yapılan tüm açıklamaları ayrıntılarıyla anlamış bulunmaktayım. Çalışmaya katılmayı isteyip istemediğime karar vermem için bana yeterli zaman tanındı. Bu koşullar altında, bana ait tıbbi bilgilerin gözden geçirilmesi, transfer edilmesi ve işlenmesi konusunda araştırma yürütücüsüne yetki veriyor ve söz konusu araştırmaya ilişkin bana yapılan katılım davetini hiçbir zorlama ve baskı olmaksızın büyük bir gönüllülük içerisinde kabul ediyorum. Bu formu imzalamakla yerel yasaların bana sağladığı hakları kaybetmeyeceğimi biliyorum. Bu formun imzalı ve tarihli bir kopyası bana verildi.

Gönüllünün (veli/vasi);

Adı- soyadı: **Telefon:**

Adres: **İmzası:**

Açıklamaları yapan araştırmacının;

Adı- soyadı: Doç. Dr. Aslı YILDIRIM **Telefon:** **İmzası:**

Rıza alma işlemine başından sonuna kadar tanıklık eden kuruluş görevlisinin;

Adı-soyadı: **Görevi:**

İmzası:

Tarih: ...../...../.....

8.2. Cirriculum Vitae

İREM DUMAN

ID No / Passport No	
Date of Birth	
Contact Address	
Phone	
e-mail	

EDUCATIONAL BACKGROUND

Country	University	Faculty/Institute	Department	Degree	Year of Graduation
Turkey	Ege University	Engineering Faculty	Bioengineering	Bachelor	2020
Turkey	Dokuz Eylul Universtiy	Izmir Biomedicine and Genome Institute	Molcular Biology and Genetics	Master's Degree	2022

ACADEMIC / PROFESSIONAL EXPERIENC

Country	City	Department	Position	Year
Turkey	Izmir	Bioengineering	Intern	Jan 2016-June 2017
Turkey	Izmir	Quality Assurance	Intern	Jul 2017- Oct 2017
Spain	Coruna	Chemistry	Intern	Jan 2018- Jul 2018
Turkey	Izmir	Novel Fluidic Technologies Laboratory	Intern	Jan 2019 - Jan 2020

Specialized Field
Tissue Engineering, Microfluidic Systems, Biomaterilas, Molecular Biology and Genetics

CONFERENCES and AWARDS

International Conferences
DUMAN, I., DEVAMOGLU, U., SAYGILI, E., YESIL-CELIKTAS, O. "Development of an Integrated Optic Sensor for Determination of B-Hydroxybutyrate within the Microfluidic Platform" Basel Life Science Fair September 2018, Switzerland
National Conferences
DUMAN, I., DEVAMOGLU, U., SAYGILI, E., YESIL-CELIKTAS, O. "Development of an Integrated Optic Sensor for Determination of B-Hydroxybutyrate within the Microfluidic Platform" TUBITAK Presentation Competition 24th & 26th June 2019
Name of The Reward
3rd Place in Bachelor Thesis Contest, Ege University Department of Bioengineering Thesis Competition Oral and Poster Presentation, 2019
3rd Place in Bachelor Thesis Contest in Aegen Area, The Scientific and Technological Research Counci l Poster Presentation Competition, 2019

PUBLICATIONS

Devamoglu, U., **Duman, I**., Saygili, E., & Yesil Celiktas, O. (2021) 2021). Development of an Integrated Optical Sensor for Determination of β Hydroxybutyrate Within the Microplatform. Applied Biochemistry and Biotechnology, 1 10.

8.3. Ethical Approval

İZMİR BİYOTIP VE GENOM MERKEZİ
GİRİŞİMSEL OLMAYAN ARAŞTIRMALAR ETİK KURULU (İBG-GOEK)
KARARI

Toplantı Tarihi	: 26/02/2021	**Toplantı Günü**	: Cuma
Toplantı Sayısı	: 3	**Toplantı Saati**	: 10:30

Sayın Doçent Sinan GÜVEN,

2021-004 Protokol No'lu; sorumlusu olduğunuz "Maküler Kornea Distrofisinin In Vitro Hastalık Modellemesi İçin 3 Boyutlu Mikroakışkan Platformun Geliştirilmesi" başlıklı araştırmanın uygulanmasında etik açıdan sakınca olmadığına oy birliği ile karar verilmiştir.

Bilgilerinizi ve gereğini rica ederiz.

Prof. Dr. H. Alper BAĞRIYANIK
Başkan

Pandemi süresince online ortamda gerçekleştirilen toplantımızda alınan kararlar tek imzalı olarak düzenlenmektedir. Pandemi sona erdikten sonra ıslak imzalı karar belgesi teslim edilecektir.